Mitochondrial genome sequencing and analysis of the invasive *Microstegium vimineum*: a resource for systematics, invasion history, and management

Craig F. Barrett[1*], Dhanushya Ramachandran[1], Chih-Hui Chen[2], Cameron W. Corbett[1], Cynthia D. Huebner[1,3,4], Brandon T. Sinn[5,6], Wen-Bin Yu[7], Kenji Suetsugu[8]

[1] Department of Biology, West Virginia University, 53 Campus Drive, Morgantown, West Virginia, USA 26506

[2] Endemic Species Research Institute, 1 Ming-Sheng East Road, Jiji, Nantou 552, Taiwan

[3] USDA Forest Service, Northern Research Station, 180 Canfield Street, Morgantown, West Virginia, USA 26505

[4] Division of Plant and Soil Sciences, West Virginia University, 204 Evansdale Greenhouse, Morgantown, West Virginia, USA 26506

[5] Department of Biology and Earth Science, Otterbein University, 1 South Grove Street, Westerville, OH USA 43081

[6] Faculty of Biology, University of Latvia, 1 Jelgavas iela, Riga, Latvia LV-1004

[7] Center for Integrative Conservation Xishuangbanna Tropical Botanical Garden, CAS Mengla, Yunnan 666303, China

[8] Department of Biology, Graduate School of Science, Kobe University, 1-1 Rokkodai, Nada-ku, Kobe, 657-8501, Japan

*Corresponding author information: Craig F. Barrett, phone: 1 (304) 293-7506, email: craig.barrett@mail.wvu.edu, ORCiD 0000-0001-8870-3672.

24

25 *Running title*: Mitogenomics of invasive *Microstegium vimineum*

26

27 *Keywords*: invasion genomics, mitogenome, long read sequencing, grass, Poaceae

28

29

30

31

Abstract

Premise of the Research. Plants remain underrepresented among species with sequenced mitochondrial genomes (mitogenomes), due to the difficulty in assembly with short-read technology. Invasive species lag behind crops and other economically important species in this respect, representing a lack of tools for management and land conservation efforts.

Methodology. The mitogenome of *Microstegium vimineum*, one of the most damaging invasive plant species in North America, was sequenced and analyzed using long-read data, providing a resource for biologists and managers. We conducted analyses of genome content, phylogenomic analyses among grasses and relatives based on mitochondrial coding regions, and an analysis of mitochondrial single nucleotide polymorphism in this invasive grass species.

Pivotal Results. The assembly is 478,010 bp in length and characterized by two large, inverted repeats, and a large, direct repeat. However, the genome could not be circularized, arguing against a “master circle” structure. Long-read assemblies with data subsets revealed several alternative genomic conformations, predominantly associated with large repeats. Plastid-like sequences comprise 2.4% of the genome, with further evidence of Class I and Class II transposable element-like sequences. Phylogenetic analysis placed *M. vimineum* with other *Microstegium* species, excluding *M. nudum*, but with weak support. Analysis of polymorphic sites across 112 accessions of *M. vimineum* from the native and invasive ranges revealed a complex invasion history.

55 *Conclusions.* We present an in-depth analysis of mitogenome structure, content, phylogenetic
56 relationships, and range-wide genomic variation in *M. vimineum's* invasive US range. The
57 mitogenome of *M. vimineum* is typical of other andropogonoid grasses, yet mitochondrial
58 sequence variation across the invasive and native ranges is extensive. Our findings suggest
59 multiple introductions to the US over the last century, with subsequent spread, secondary
60 contact, long-distance dispersal, and possibly post-invasion selection on awn phenotypes. Efforts
61 to produce genomic resources for invasive species, including sequenced mitochondrial genomes,
62 will continue to provide tools for their effective management, and to help predict and prevent
63 future invasions.

Introduction

Invasive species cause damage to natural, agricultural, and urban ecosystems, equating to billions of dollars (USD) in economic and environmental loss (Pimentel et al., 2005; Simberloff et al., 2013). Such problems have been exacerbated by climate change and greater interconnectedness across the globe (Finch et al., 2021). Genomic resources provide practitioners and researchers with a baseline of powerful tools in medicine, agriculture, and virtually all areas of the life sciences, yet such tools are generally lacking for invasive species compared to those in crop and animal systems (Matheson and McGaughran, 2022). However, the widespread availability and increasing affordability of genome sequencing technologies and bioinformatic platforms are changing the landscape of invasion biology (North et al., 2021). For example, such advances in genomics are allowing more nuanced reconstructions of invasion history (van Boheemen et al., 2017; Sutherland et al., 2021; Bieker et al., 2022), linking of genotypic and phenotypic variation (Turner et al., 2021; Revolinski et al., 2022), epigenetics (Banerjee et al., 2019; Mounger et al., 2021), and forecasting of potential future invasions (Hudson et al., 2021).

Generally speaking, plant mitochondrial genomes ('mitogenomes') have experienced less attention than plastid or nuclear genomes (Mower et al., 2012). This is largely due to their extensive variability in structural dynamics and repetitive DNA content, making them difficult targets for complete genomic sequencing (Palmer and Herbon, 1988; Alverson et al., 2010). This is in contrast to animal mitogenomes, which evolve rapidly in terms of substitution rates but are more structurally conserved. In combination with their smaller size (10-20 kb in animals vs. 100 kb to > 10 Mb in plants; Gualberto et al., 2014), animal mitogenome sequencing is more

straightforward than in plants, making animal mitogenomes significantly better represented across the Tree of Life. Improvements in long read sequencing technology, however, have rekindled interest in plant mitochondrial genomics, allowing the assembly of complete or nearly complete mitogenomes, which often display repetitive regions and structural isoforms making them difficult or impossible to assemble with short-read technologies (Kovar et al., 2018; Jackman et al., 2020). Analyses of plant mitogenomes have revealed an array of structures, including circular genomes, “master circles” with sub-stoichiometric circular structures, linear structures, multi-chromosomal structures, and branched structures (Bendich, 1993; Sloan, 2013; Wu et al., 2015; 2022).

Plant mitogenomes typically contain 50-60 genes, including those encoding protein products (CDS, or coding DNA sequences), transfer RNAs (tRNAs), and ribosomal RNAs (rRNAs) (Gualberto et al., 2014). They are also known to contain plastid-like regions, likely as remnants of both ancient and recent intergenomic transfers and gene conversion events, representing up to 10.3% of the mitogenome in the date palm *Phoenix dactylifera* (Fang et al., 2012). Additionally, plant mitogenomes have been demonstrated to house foreign DNA, possibly remnants of ancient or more recent close biotic interactions (e.g. Rice et al., 2013; Sanchez-Puerta et al., 2019; Sinn and Barrett, 2020; Lin et al., 2022).

Grasses are overrepresented in terms of complete mitogenomes among plant families, with 67 complete genomes in NCBI GenBank, though more than half of these comprise multiple accessions of a few crop species (e.g. *Hordeum vulgare, Oryza sativa, Triticum aestivum, Zea mays*; last accessed 18 November, 2022). However, grasses are also overrepresented among

invasive plant species (Daehler, 1998; Kerns et al., 2020), allowing for meaningful comparisons among invasive and non-invasive species within this ecologically and economically important family. Only a handful of mitogenomes have been sequenced for invasive plants, and most are grasses [e.g. *Silene vulgaris* (Caryophyllaceae); *Chrysopogon zizianoides*, *Coix lacryma-jobi*, *Eleusine indica*, and *Lolium perenne* (Poaceae)]. Thus, studies of mitochondrial genome dynamics in invasive plants, and potential applications in their effective control, are in their infancy. For example, a simulation study by Hodgins et al. (2009) explored the possibility of incorporating cytoplasmic (mitochondrial) male sterility alleles in the control of invasive plants by limiting pollen production. Yet, empirical data and sequenced reference mitogenomes are too few to test the effectiveness of such approaches more broadly in invasive plant species, nearly all of which can be categorized as non-model species.

Microstegium vimineum (stiltgrass) is an aggressive, established invader of eastern North American forest ecosystems, and is one of the most damaging invasive species on the continent (e.g. Huebner, 2010a; Johnson et al., 2015). Likely introduced as packing material for porcelain in the early 1900s (Fairbrothers and Gray, 1972), this species has spread to 30 US states, and is expanding into Canada, the northeastern US, and the northern US Midwest (Huebner, 2010a; 2010b; Mortensen et al., 2009; Rauschert et al., 2010; Barrett et al., 2022). Further, it is hypothesized that *M. vimineum* was introduced multiple times in the US, first in the southeastern US, and later in the Northeast, with subsequent spread and secondary contact, providing an apt case study in the genomic dynamics of the invasion process (Novy et al., 2013; Barrett et al., 2022). Recently published plastid and nuclear genomes are now available for this species (Welker et al., 2020; Ramachandran et al., 2021, respectively), but a complete mitogenome is

lacking. Therefore, the objective of this study is to assemble a reference mitogenome for *M. vimineum*, with the goal of aiding studies of invasion history, evolution, ecology, and management. We explore genome structure and content, phylogenetic relationships of *Microstegium*, and patterns of mitogenomic variation across the native and invasive ranges with respect to invasion history in *M. vimineum*.

Materials and Methods

Organellar genome sequencing and assembly

Leaf material was sampled from a growth chamber-grown accession (seed from Potomac Ranger District, Monongahela National Forest, West Virginia, USA), flash-frozen in liquid Nitrogen, and stored at -80C. DNAs/RNAs were extracted, and PacBio (DNA) and Illumina (DNA and RNA) sequencing were conducted as described in Ramachandran et al. (2021). The software seqtk v.1.0-r31 (https://github.com/lh3/seqtk) was used to randomly subsample PacBio reads (400,000 reads). MegaBLAST from the NCBI BLAST+ suite (Camacho et al., 2008) was conducted with the subsampled read pools against the mitochondrial genome of *Sorghum bicolor* (NCBI GenBank number NC_008360) in Geneious v.10.0.9 (http://www.geneious.com/), specifying an e-value of $1e^{-5}$, and binning into 'hits' vs. 'no hits,' keeping only reads >20 kb in length. The resulting positive BLAST hits for each set were then assembled with CANU v.2.2 under default parameters (Koren et al., 2017). The resulting graphs from CANU (.gfa files) were inspected in BANDAGE v.0.9.0 (Wick et al., 2015) to visualize contiguity and coverage of the assemblies. Resulting scaffolds were further assembled into a single scaffold in Geneious using

the native overlap-layout-consensus '*de novo* assembly' option. Mitochondrial and plastid contigs were identified using the live annotation feature in Geneious, with the annotations from *Sorghum bicolor* (mitochondrial), and an accession of *M. vimineum* (plastome; accession TK124, GenBank number MT610045) at a 70% threshold, respectively. Circlator was used to attempt to circularize the scaffold (Hunt et al., 2015).

Mitochondrial and plastid contigs were extracted separately as FASTA files. FLYE was then used to correct the mitochondrial and plastid scaffolds with ten polishing iterations using the PacBio data (Kolmogorov et al., 2019). The assembly was further polished with Illumina data using PILON (Walker et al., 2014). Illumina data (8,605,412 read pairs from accession WV-PRD-2-4, the same collection used for PacBio sequencing) were trimmed with BBDUK v.38.51 (https://sourceforge.net/projects/bbmap) to remove Illumina adapters, low quality bases (minimum quality = 6), and low-complexity regions (minimum entropy = 0.5, maximum GC content = 0.9). Illumina reads were then mapped to the organellar assemblies with NGM (Sedlazeck et al., 2013) to output a .sam alignment file. The .sam file was then sorted and indexed with SAMTOOLS v.1.7 (Li et al., 2009). The PacBio assemblies and sorted .bam file were then used for error correction/polishing with PILON.

The resulting polished FASTA file was imported into Geneious and annotated using the 'live annotation' feature, at a 75% similarity threshold, using the mitochondrial annotations from *Coix lacryma-jobi* var. *ma yuen* (GenBank accession number MT471100), *Sorghum bicolor* (same accession as above), *Oryza sativa* (ON854123), *Zea mays* (CM025451), and *Saccharum officinarum* (MG969496) and the plastid annotation from *Microstegium vimineum* (same as

179 above). Annotations were then checked visually to confirm proper start/stop codons and to
180 investigate the presence of premature stop codons, suggesting mis-annotations. The annotation
181 was exported from Geneious as a GenBank Flat File and converted to a feature table with
182 GB2Sequin (Lehwark and Greiner, 2019) via the ChloroBox portal (https://chlorobox.mpimp-
183 golm.mpg.de). The resulting feature table was downloaded and manually edited to ensure the
184 correct orientation of exons in genes containing them. The annotation (feature table + fasta file)
185 was then submitted to GenBank though the BankIt web portal
186 (https://www.ncbi.nlm.nih.gov/WebSub).
187
188 *Analyses of repetitive DNA, plastid-like DNA, RNA editing, and structural variation*
189
190 Geneious was used to identify large, identical repeats >1,000 bp, using the native Repeat Finder
191 plugin (https://www.geneious.com/plugins/repeat-finder/) as well as the self-dotplot function,
192 with a window size of 500 bp and tile size of 100 kb. REPuter (Kurtz et al., 2001; via
193 https://bibiserv.cebitec.uni-bielefeld.de/reputer/) was further used to detect repetitive regions >8
194 bp in length in forward, reverse, reverse-complement, and palindromic configurations (edit and
195 Hamming distances = 0). Plastid-like regions were identified by annotating the mitogenome with
196 all plastid genes from *M. vimineum* (Genbank # MT610045) in Geneious at a 60% similarity
197 threshold, in order to detect degraded or pseudogenized plastid-like sequences. Further, to
198 identify plastid-like regions not corresponding to annotated genes, Illumina reads from accession
199 WV-PRD-2-4 (same as above) were mapped to the reference mitogenome to identify putative
200 plastid-like regions with higher than expected coverage depth. These regions were annotated in
201 Geneious as having >3x standard deviations in coverage depth relative to the rest of the genome.

RNAseq reads from the same collection from young, developing leaf tissue (NCBI Sequence Read Archive accession SRX12501806), were mapped to the reference genome using the Geneious read mapper for RNAseq data, and SNPs were called to identify putative RNA editing sites for all CDS (e.g. C → U). Minimum required coverage depth for a SNP was 10×, further requiring a minimum variant frequency of 0.9, such that only variants that differed among the RNAseq and DNAseq data were identified (i.e. the polished reference). Relative expression levels (transcripts per million, TPM) were calculated in two ways. First, all RNAseq reads were mapped to the plastome to filter plastid reads in Geneious, then the remaining reads were mapped to the mitochondrial annotation to quantify expression levels of all mitochondrial coding sequences (CDS). Then, the plastid-like region annotations were overlaid on the mitochondrial genomes, and plastid-filtered reads were mapped to assess whether plastid-like regions of the mitogenome displayed evidence of expression. All results were plotted in R with the packages dplyr v.1.0.10 (Wickham et al., 2023), ggplot2 v.3.3.6 (Wickham, 2016), and ggpubr v.0.4.0 (Kassambara, 2020). To investigate variation in mitogenome structure, eight random subsets of 200,000 PacBio reads were sampled with Seqtk and BLASTed against the *Sorghum* mitogenome (as above). BLAST hits were assembled with Flye, and the longest mitochondrial contigs were mapped to the reference genome model with the LASTZ v.1.04.22 (Harris, 2007) plugin for Geneious.

Identification of transposable elements and foreign-aquired sequence

RepeatMasker version 4.1.1 (Smit et al., 2013) was used to discover and identify transposable elements (TEs) in the mitogenome assembly, usingRepBase-20181026 database of Viridiplantae (Bao et al., 2015) and a custom set of 1,279 *M. vimineum* consensus repeat sequences (Ramachandran et al., 2021). Additional repeat identification tools were used to screen for the presence of partial or truncated TE sequences in the mitogenome. HelitronScanner (Xiong et al., 2014) was used to identify helitrons using 5′ and 3′ terminal motifs. Miniature inverted-repeat transposable elements (MITEs) were detected using the program MiteFinderII (Hu et al.,2018) under default settings.

Kraken 2 (v.2.1.2; Wood et al., 2019) was used to screen for the presence of interspecific genomic transfers, excluding those from the plastome. The mitogenome assembly, with repeats masked and plastid sequences removed, was decomposed into 100 bp segments using the reformat.sh script of the BBMAP suite (https://sourceforge.net/projects/bbmap/). The k-mers contained in the resulting 4,292 sequences were classified via screening against to precompiled Kraken 2 databases (available via: https://benlangmead.github.io/aws-indexes/k2): 1) PlusPFP database, which contained the complete genomes of plants, bacteria, archaea, viruses, fungi, human and UniVec vectors accessioned in NCBI's RefSeq database; 2) sequences from 389 species in the Eukaryotic Pathogen, Vector and Host Informatics Resource Database (Amos et al., 2022). The NCBI Taxonomy (accessed 8 September 2022) was used for the annotation of classified sequences. The default values for k-mer length (35) and minimizer value (31) were used.

Phylogenomic analyses using mitochondrial CDS

Mitochondrial genomes and mitochondrial protein coding sequences were downloaded from NCBI Genbank using the search terms 'Poales,' 'mitochondrion,' and 'complete.' *Cocos nucifera* (NC_031696) and *Phoenix dactylifera* (NC_016740) were chosen as outgroups, as both are members of the palm family (Arecales) and the 'commelinid' clade, to which Poales also belongs. Sequence annotations were extracted from Geneious and aligned with the codon-aware aligner MACSE v.2 (Ranwez et al., 2018). Alignments were then concatenated in Geneious, and sites with > 10% missing data were excluded (File S1). The final alignment was analyzed with maximum likelihood under the 'GHOST' heterotachy model (Crotty et al., 2020) in IQTree2 (Minh et al., 2020), which allows mixed substitution rates and branch lengths. This model is especially appropriate for lineages such as Poales, which have been shown in previous studies to exhibit heterotachy in phylogenomic estimates based on organellar DNA (e.g. Givnish et al., 2010; Barrett et al., 2016). This model approach avoids the need to partition the data by gene and codon, and can accommodate changes in substitution rates across branches and time. IQTree2 was run under the GHOST model with 1,000 ultrafast bootstrap pseudoreplicates (Hoang et al., 2018). The resulting tree file was visualized in FigTree v.1.4.4 (http://tree.bio.ed.ac.uk/) and edited with Adobe Illustrator v. 26.5 (Adobe, Inc., 2023).

Assessment of relationships among mitochondrial haplotypes of M. vimineum

To characterize haploid single nucleotide polymorphisms (SNPs) in the mitogenome, we sampled 112 accessions from both the invasive (N = 74) and native ranges (Asia, n = 38), plus six accessions from different species of *Microstegium* as outgroups. Samples were either field

collected in 2019-2020 (n = 66), or from herbarium specimens (n = 46) dating back to 1934 (Appendix A1). Total genomic DNAs were extracted via the CTAB method (Doyle and Doyle, 1987), and quantified via Qubit Broad Range DNA assay (Thermo Fisher Scientific, Waltham, Massachusetts, USA). DNAs were further visualized on a 1% agarose gel to assess degradation and diluted to 20 ng/ul with nanopure water. Illumina sequencing libraries were prepared with the SparQ DNA Frag and Library Kit at 2/5 volume (Quantabio, Beverly, Massachusetts, USA), which uses a fragmentase to shear genomic DNA, followed by end repair and adapter ligation. The shearing step for herbarium-derived DNAs was reduced to 1 min from 14 min, as these all showed some level of fragmentation prior to library preparation. Libraries were then amplified with primers matching the adapter sequences, adding dual-indexed barcodes (12 PCR cycles). Final library concentrations were determined via Qubit High Sensitivity DNA assay and pooled at equimolar ratios. Library pools were sequenced on two runs of 2 × 100 bp Illumina Nextseq2000 (v.3 chemistry) at the Marshall University Genomics core with samples from other studies, producing a total of ~1 billion read pairs per run.

Reads were processed using a dedicated SNP calling pipeline (https://github.com/btsinn/ISSRseq; with scripts available at https://zenodo.org/record/5719146#.Y-EvfnbMKHs; Sinn, Simon et al., 2022). Briefly, reads were trimmed and filtered with BBDUK (http://sourceforge.net/projects/bbmap), with minimum read quality = PHRED 20, entropy and low complexity filters set to remove reads with < 0.1 or > 0.9 % GC content, kmer length set to 18, and the ‘mink’ flag set to 8. The reference genome was indexed and reads were mapped with BBMAP (https://sourceforge.net/projects/bbmap/). Here, plastid-like regions and one copy of each large repeat were removed from the reference genome

to minimize drastic differences in coverage depth and plastid SNPs being misinterpreted as mitochondrial SNPs. The resulting .bam files were sorted and PCR duplicates were removed with PICARD (version 2.22.8; Broad Institute). SNPs were called with GATK HaplotypeCaller (Poplin et al., 2017) following GATK best practices (Van der Auwera et al., 2013; Van der Auwera and O'Connor, 2020), here with ploidy = 1, resulting in .vcf files for all raw and GATK-filtered variants. The filtered .vcf was then converted to .nexus format with vcf2phylip (Ortiz, 2019), keeping only sites represented in at least 12 accessions (File S2). Phylogenetic analysis was conducted as above, with the exception that the GHOST heterotachy model was not used (as variation below the species level should not be expected to show strong patterns of heterotachy). Instead, the best-fit model was selected from the entire dataset using ModelFinder (Kalyaanamoorthy et al., 2017) under the Bayesian Information Criterion (BIC).

The annotated mitogenome sequence for *M. vimineum* was deposited in NCBI GenBank under accession OQ360108. Raw read data used to build the genome (PacBio, RNAseq), for phylogenomics, and for SNP analysis (DNAseq) was deposited in the NCBI Sequence Read Archive under BioProject PRJNA769079. Supplementary files are available at https://doi.org/10.5281/zenodo.7618370.

Results

Organellar genome sequencing and assembly

316 The final, polished assembly was 478,010 bp in length (Fig. 1A), with overall GC content at
317 43.7% (41.3% for protein-coding sequences, 53.0% for rRNA genes, and 51.1% for tRNA
318 genes). The initial assembly resulted in six contigs, three of which comprised the plastid genome
319 (large and small single copy regions, inverted repeat), and three of which comprised the
320 mitogenome. The latter were assembled into a single contig based on overlapping ends with the
321 Geneious *de novo* assembler. Despite attempts to circularize the genome with Circlator, a single,
322 "master circle" model could not be constructed. The final genome assembly contained two large,
323 inverted repeats and a single, large, direct repeat: IR1 (28,247 bp), IR2 (2,380 bp), and DR1
324 (6,462 bp), respectively. Potential secondary structures of the genome model are depicted in Fig.
325 1B and C. One possible secondary structure (Fig. 1B) consists of large and small single copy
326 regions (which contain copies of IR2 and DR1) and a large IR(1). Another possible structure,
327 considering both large IR sequences, consists of three single copy regions, separated by the two
328 IRs (Fig. 1C). Mean coverage depths of the three regions from Fig. 1B are: 31x (PacBio) and 42x
329 (Illumina) for IR1; and 23x (PacBio) and 21x (Illumina) for the both "single copy" regions.
330
331 *Analyses of repetitive DNA, structural variation, plastid-like DNA, RNA editing, transposable*
332 *elements, and foreign-acquired sequences.*
333
334 The genome assembly contains 32 protein-coding genes (CDS), three ribosomal RNA genes
335 (*rrn*), and 27 transfer RNA genes (*trn*). In addition to the large repeat regions above, the
336 mitogenome of *M. vimineum* contains numerous smaller repeats (< 1,000 bp). These include
337 direct repeats (880 bp, 262 bp, 164 bp, and 109 bp), inverted repeats (165 bp, 109 bp), and one
338 repeat with three intervals of 154 bp (forward, forward, reverse). The genome contains eight

tandem repeat regions: $(AC)_6$, $(AG)_6$, $(AT)_{10}$, $(CT)_6$, and $(ACTTT)_5$, and three regions of $(AT)_7$. Further, it contains 87 dispersed repeats < 100 bp in length in forward/forward orientation (mean length = 36.3 bp) and 101 in forward/reverse orientation (mean length = 35.0 bp). Comparison of repeat content with relatives of *M. vimineum* within tribe Andropogoneae reveal similar patterns (Fig. 2A): large inverted repeats (i.e. > 5 kb) are present in *M. vimineum* (2), *Chrysopogon zizanioides* (3), and *Coix lacryma-jobi* (4). The same is true for large direct repeats, which are present in all species: *Microstegium* (1), *Chrysopogon* (1), *Coix* (2), *Saccharum* (1), and *Sorghum* (2). LastZ alignments revealed seven different structural conformations of the *M. vimineum* mitogenome based on assemblies from eight random subsets of 200,000 PacBio reads (Fig. 2B). Nearly all of the apparent breakpoints were associated with large direct or inverted repeat regions, while one major breakpoint was associated with a small (109 bp) direct repeat.

Plastid-like sequences comprise 2.4% of the genome. In total, successfully transferred annotations of plastid genes to the mitogenome comprised 43 annotations, 17 of which were CDS (Fig. 3) and the remainder of which were tRNA-like genes. Average percent similarity for CDS was 78.53 (range = 39.7) and for *trn*-like regions was 76.01 (range = 39.2). The three largest annotated plastid-like regions in the *M. vimineum* mitogenome correspond to *atpB*, *psaB*, and *rpoC1*, with percent similarities to their plastomic homologs of 75.3, 73.6, and 70.9, respectively (Fig. 3). Several plastid-like sequences are also found in the mitogenomes of other members of tribe Andropogoneae, and more broadly among grasses, including *atpB, atpE*, *ndhK*, *psaB*, *psbF*, *rpl14*, *rpl2*, *rpl23*, *rpoC1*, *rps19*, and *rps2*. All plastid-like mitochondrial regions in *M. vimineum* showed evidence of pseudogenization relative to their plastid-encoded homologs, including high levels of divergence, 5’ or 3’ truncation, internal stop codons, and frameshift

362 insertions or deletions. The only region with an intact reading frame corresponded to *atpE*,
363 having three substitutional differences relative to the plastid copy; two of these were adjacent
364 and resulted in replacements at codons 3 and 4 (L → F and N → H, respectively).
365
366 Analyses of gene expression based on RNA-seq data from developing leaf tissue revealed that
367 over half of all expressed mitochondrial transcripts were ATP Synthase (*atp*, TPM range =
368 33,500.5-329,781.1) (Fig 4A, B), followed by Cytochrome C Oxidase (*cox*, TPM = 30,052.4-
369 67,602.3) and NADH Dehydrogenase (*nad*, 5,668.2-50,473.9) (Fig. 4A, B). Expression was also
370 detected for plastid-like regions, predominantly *ndhK* (TPM = 654,340.2) and *psaJ* (142,073.1)
371 (Fig. 4C). Together, these two regions accounted for >75% of all putatively expressed, plastid-
372 like regions, despite the former having multiple internal stop codons and the latter being
373 truncated at the 3' end. There was evidence of C → U RNA editing among mitochondrial CDS
374 as well, ranging from 1 site per gene to 18 sites per gene (*viz*. *ccmC*; Fig.4D). The vast majority
375 of RNA editing involved replacement substitutions, with SER → LEU being the most common
376 type (Fig. 4E).
377
378 Searches for transposable element-like (TE-like) sequences recovered 29 hits in RepeatMasker,
379 including sequences similar to Class I retrotransposons (n = 14) and Class II DNA transposons (n
380 = 10; Fig. S1). Class I retrotransposon-like sequences belonged to LTR/Copia (n = 4; length
381 range = 102-646 bp), LTR/Gypsy (n = 9; 44-1,313 bp), and LINE/L1 Superfamilies (n = 1; 108
382 bp). Among Class II DNA transposon-like sequences, nine were similar to DNA/PIF-Harbinger
383 (47-6,881 bp), two of which were > 6 kb in length (Fig. S1). Another Class II-like sequence
384 corresponded to the DNA/CMC-EnSpm superfamily (139 bp). Five TE-like hits were

385 unclassified, ranging from 32-2,437 bp in length. Additional searches with HelitronScanner
386 found three hits for Helitron-like sequences, of 571, 14,875, and 5,477 bp. The first was
387 identified in the spacer region between *rps12* and *ccmB*, the second between *nad4* and *nad1*
388 intron 3, and the third overlapping with *cox1*. MiteFinderII found three hits of MITE-like
389 sequences with length of 246, 400, and 285 bp. The first was identified between *trnS-GGA* and
390 *rps7*, the second between *trnP-TGG* and *nad5* (exon 5), and the third between *ccmFC* and *trnK-*
391 *TTT* (which is duplicated within the largest inverted repeat region). Taken together, 9.05% of the
392 *M. vimineum* mitogenome is composed of TE-like sequences.
393
394 Analysis of the mitogenome assembly with Kraken2 supports a genome which is free from
395 foreign sequences and contamination (Fig. S2). Scanning of k-mers comprising 100 bp segments
396 of the mitogenome against those found in genomes representing plants, bacteria, archaea,
397 viruses, fungi, UniVec contaminants, and the human genome resulted in classification of 77.52%
398 of k-mers, of which 77.45% were classified as characteristic of k-mers optimized to the node
399 representing the hypothesized ancestor of Viridiplantae, 74.44% of Liliopsida, and 72.3% as
400 Poaceae. The remaining unclassified k-mers either represent our incomplete knowledge of
401 mitogenomic diversity or the presence of sequences unique to the mitogenome of this species.
402
403 *Phylogenomic analyses using mitochondrial CDS*
404
405 Analysis of 7,019 aligned positions across 28 protein-coding mitochondrial genes (total
406 gaps/missing data content = 7.2 %, total parsimony-informative characters = 1,955) under the
407 GHOST heterotachy model yielded a tree topology with generally high bootstrap support values

(lnL = -31,900.1643, BIC score = 65,013.6522, total branch/model free parameters = 137; Fig. 5A). Among the families of order Poales, mitochondrial data placed Typhaceae as sister to Bromeliaceae + the remainder of the order (BS = 99). In the latter clade, Xyridaceae were sister to a clade composed of ((Mayacaceae, (Thurniaceae, Cyperaceae, Juncaceae)), (Joinvilleaceae, Poaceae)); all BS = 100 excluding the sister relationship of (*Mayaca, Xyris*) (BS = 47) and Mayacaceae as sister of (Thurniaceae, Cyperaceae, Juncaceae) (BS = 77). Within Poaceae, *Puelia* (Puelioideae) was supported as sister to the remaining taxa (BS = 100), followed by representatives of tribes Bambusoideae (*Bambusa*, *Ferrocalamus*) and tribe Pooideae (e.g. *Lolium*, *Triticum*, *Thinopyrum*, *Hordeum*), but with a lack of support for the latter subfamilies as sister to one another (BS = 48). Following this, Oryzoideae (*Oryza*) (BS = 100) was placed as sister to Chloridoideae (*Eleusine*, BS = 100), and Panicoideae (BS = 100). Within Panicoideae, *Alloteropsis* was sister to a clade comprising members of the subtribe Andropogoneae (BS = 99). Within Andropogoneae, (*Tripsacum*, *Zea*) were sister to a clade composed of *Sorghum*, *Microstegium*, *Saccharum*, *Chrysopogon*, and *Coix* (BS = 100), with BS = 92 for the latter. However, support was generally low within this clade. *Microstegium nudum* was placed as sister to two accessions of *Sorghum*, but with no support (BS = 52). Sister to this clade is a clade of (*Coix*, *Microstegium*), but again, with no support (BS = 46). Among the remaining accessions of *Microstegium*, *M. faurei* was sister to the rest but with no support (BS = 52), while *M. vimineum* was placed as sister to *M. japonicum* and an unknown accession of *Microstegium* from Yunnan, China (BS = 100); the latter specimen was 100% identical to *M. japonicum*.

Assessment of relationships among mitochondrial haplotypes of M. vimineum

Analysis of genome skim datasets for 118 accessions from the US (invasive) and Asia (native) yielded 3,913 mitochondrial variants. Phylogenetic analysis of the data in IQtree2 yielded a tree with two principal clades corresponding to samples from the invasive range (best-fit model = SYM+ASC+R5, lnL = -47,277.03, BIC score = 96,588.99, total branch/model free parameters = 246; Fig. 5B). These two clades were sister to a clade of haplotypes from Japan (from Fukuoka, Shiga, and Shizuoka), collectively sister to a single haplotype from Nantou, Taiwan. The first clade containing accessions from the invasive range was primarily composed of individuals from the southeastern USA that lack awns (BS = 91). Interspersed among these invasive-range accessions were several accessions from Japan. Bootstrap values among individual haplotypes within this clade were generally low. The second clade was composed of primarily awned forms from the northeastern US, but this clade as a whole received weak support (BS = 67). Invasive haplotypes in this clade were interspersed among those from Japan and Taiwan, with a single haplotype from China; likewise, support values were generally low within this clade. There were exceptions, however: four haplotypes from Tompkins County, New York, USA grouped with the predominantly "southern" clade (predominantly southern US awnless accessions), whereas six haplotypes from eastern Tennessee, southern West Virginia, southern Ohio, and southern Illinois, USA grouped with the predominantly "northern" clade.

Discussion

Organellar genome sequencing and assembly

We sequenced and analyzed the 478,010 bp mitochondrial genome of the invasive *M. vimineum*, revealing a genome typical of previously sequenced grasses. Grass mitogenomes represented in NCBI GenBank range from 294 to 740 kb (last accessed January, 2023), thus *M. vimineum* has a somewhat average genome size with gene content typical of other grasses. Overall, gene space occupies 13.2% of the genome, followed by TE-like sequence (9.05%) and plastid-like sequence (2.4%), leaving 75.3% as unknown.

Analyses of repetitive DNA, structural variation, plastid-like DNA, RNA editing, transposable elements, and foreign-acquired sequences

As observed in other mitogenomes, both large (i.e > 1,000 bp) and small direct and indirect repeats are present in *M. vimineum* (Figs. 1, 2). Further, these repeats are associated with putative isomeric variants, which argues against the existence of a “master circle” (Figs. 1, 2; Sloan, 2013). In fact, the genome could not be circularized with PacBio or Illumina reads, casting further doubt on the existence of a single circular structure. Insertions of plastid-like DNA regions, many of which are divergent from their homologs in the plastid genome of *M. vimineum*, suggests that many of these regions may be considered “ancient” transfers, while some others may have either occurred more recently or are the result of “copy correction” via gene conversion (Fig. 3A; Sloan and Wu, 2014). The total extent of plastid DNA content detected in the mitogenome species is not extreme (2.4% compared to > 10% in the palm *Phoenix dactylifera*; Fang et al., 2012), but is similar to that in other grasses (e.g. Clifton et al., 2004). The apparent expression of some of these regions presents a conundrum, as our evidence suggests these are non-functional, lacking intact open reading frames. One possible explanation

would be that these plastid-like regions lie within expressed cistrons, and thus are transcribed but potentially spliced out or their RNAs modified post-transcription (Cardi et al., 2012). Previous research has shown that most of the mitogenome can be transcribed, and that extensive post-transcriptional modification produces the mature transcripts (Holec et al., 2006; Ruwe et al., 2016). RNA editing was also observed within CDS of *M. vimineum*, a common feature of both organellar genomes in plants; this process is likely essential for proper gene expression and further may preserve the integrity of secondary structure in organellar genomes (e.g. Maier et al., 1996). It should be noted that only a single tissue type (young developing leaf tissue) from a single individual was included here, and thus the need remains for gene expression studies across tissue types, developmental stages, and environmental conditions to explore the transcriptional landscape in this invasive species.

Integration of nuclear-derived TE-like sequences provide a partial explanation for plant mitochondrial genome size expansion (Marienfeld et al. 1999, Mower et al. 2012, Zhao et al. 2018). Previous research on *Arabidopsis thaliana*, *Citrullus lanatus*, *Cucurbita pepo*, *Lingustrum quihoui* and, *Elymus sibiricus* have reported ~1-6% of nuclear-derived TE-like sequences in their respective mitogenomes (Knoop et al. 1996, Alverson et al, 2010, Yu et al. 2020, Xiong et al. 2022). Although 9.05% of the mitogenome of *M. vimineum* is occupied by similar TE-like sequences (Fig. S1), the majority of them are fragmented copies. These results indicate frequent and independent DNA transfers from nuclear to mitochondrial genome, that the fragmented copies could have either been generated from former complete sequences that later became degraded, they originated from incomplete transposition events, or they were scrambled by intramolecular recombination which is frequent in plant mitogenomes (Knoop et al. 1996, Notsu

et al. 2002). Regardless, the landscape of TE-like sequences in plant mitogenomes is not well explored.

An absence of sequence from distantly related plant lineages, or other lineages in general, suggests that the mitogenome of *M. vimineum* is free of foreign sequence, foreign sequence is too recombined to identify, or k-mers present are highly unique and are not contained in the genomes included in our analyses (Fig. S2). We find the latter two explanations unlikely, given the broad range of lineages represented in our Kraken2 databases. Additionally, none of the k-mers from our assembly were classified when searched against the Eukaryotic Pathogen, Vector and Host informatics Resource Database. Taken together, these results characterize a mitogenomic assembly which is free of confounding artifactual contamination resulting from interactions in the lab or during necessary bioinformatic components of our work.

Phylogenomic analyses using mitochondrial CDS

Microstegium species, including *M. vimineum*, are clearly placed within the grass tribe Andropogoneae based on mitochondrial data (Fig. 5A). Our analysis of mitochondrial coding regions suggests a close relationship among most of the *Microstegium* species sampled here, with the exclusion of *M. nudum*, and possibly *M. faurei*; the latter was placed as sister of *M. ciliatum*, *M. glaberrimum*, *M. japonicum*, and *M. vimineum*, but with no support. This is in contrast to other studies based on plastid DNA in which species of *Microstegium* occupy different clades within the Andropogoneae, though the level of *Microstegium* spp. sampling in those studies, and the lack of available mitogenomes across Andropogoneae in the current study,

522 are insufficient for confident placement of the different species. Lloyd Evans et al. (2019) placed
523 *M. vimineum* with moderate support as sister to *Polytrias* and two species of *Sorghastrum*, all of
524 which are sister to a clade composed of *Miscanthus* and *Saccharum* spp. based on five low-copy
525 nuclear genes. In that study, *M. vimineum* is estimated to have diverged from a common ancestor
526 with *Polytrias* and *Sorghastrum* between 7 and 10.5 million years ago, but sampling only
527 included *M. vimineum* from the genus *Microstegium*. Data from complete plastid genomes
528 placed *M. vimineum* as sister to two genera: *Kerriochloa*, with a single species *K. siamensis*
529 (Thailand, Vietnam); and *Sehima*, comprising five species from Africa, Asia, and Australia
530 (Welker et al., 2020). But again, *M. vimineum* was the only representative of *Microstegium*
531 sampled.
532
533 Chen et al. (2009; 2012) conducted a phylogenetic analysis and taxonomic treatment of
534 *Microstegium* based on nuclear ITS sequencing and morphology. Our findings of *M. nudum* as
535 sister of *Sorghum*, with other species of *Microstegium* occupying a different clade (more closely
536 allied with *Coix*) are generally in agreement with these previous studies, but with some key
537 differences. First, Chen et al. (2012) identify two clades, a '*M. nudum*' clade (*japonicum*, *nudum*,
538 *somae*), and a '*M. vimineum*' clade (*ciliatum*, *faurei*, *geniculatum*, *vimineum*). In our
539 phylogenetic analysis, only *M. nudum* grouped outside the main clade of *Microstegium*, but
540 support overall for the latter is weak (Fig. 5A). In our analysis, *M. vimineum* was strongly
541 supported as sister to *M. japonicum* and an unknown species of *Microstegium* (BS = 100),
542 whereas the analysis of Chen et al. (2012) placed *M. vimineum* as sister to *M. ciliatum*, but with
543 low support (BS = 69). While the taxon sampling of mitogenomes in the current study is not

544 comprehensive, it does represent the largest amount of data analyzed to date on the taxonomic
545 status of the genus.
546
547 Based on our analysis and previous studies, it is indeed possible that *Microstegium* is non-
548 monophyletic, perhaps reflecting a complex, reticulate history of allopolyploidy that is broadly
549 observed among the Andropogoneae (e.g. Estep et al., 2014; Hawkins et al., 2015; Arthan et al.,
550 2017; Ramachandran et al., 2021). *Microstegium vimineum* is a known polyploid, with 2N = 20
551 chromosomes, twice that of the "base" number of 2N = 10 in Andropogoneae (Watson and
552 Dallwitz, 1992). Further, analysis of the recently published chromosome-level nuclear genome of
553 *M. vimineum* revealed strong evidence of a paleopolyploidy event, with about 1/3 of all nuclear
554 genes present as duplicate copies (Ramachandran et al., 2021). Further, comparative analysis of
555 terminal repeats of transposable elements throughout the nuclear genome, calibrated to a grass-
556 specific TE divergence rate (Ma and Bennetzen, 2004), revealed a burst of TE activity roughly 1-
557 2 million years ago, possibly coinciding with "genomic shock" associated with a polyploidy
558 event (Ramachandran et al., 2021). This warrants further study with dense taxon sampling across
559 the tribe, including multiple species and accessions of *Microstegium*, and employing genome-
560 wide plastid, mitochondrial, and nuclear markers to test hypotheses of allopolyploid origins
561 within the currently circumscribed *Microstegium* and other genera.
562
563 *Assessment of relationships among mitochondrial haplotypes of* M. vimineum
564
565 Patterns of mitogenomic SNP variation within *M. vimineum* reveal a complex invasion history
566 (Fig. 5B). The finding of a predominantly "northern awned" clade and a "southern awnless"

clade mirrors that based on nuclear SNP data (Barrett et al., 2022) and plastid data (Corbett C. W. et al., unpublished data). Further, there is evidence of multiple invasions and subsequent establishments from the native range, with a likely initial, successful "awnless" invasion in the southeastern US and at least one more successful invasion in the northeastern US of the awned form, likely in eastern Pennsylvania. Because this species was used as packing for shipments from Asia, it is plausible for multiple invasions to have occurred, perhaps bearing higher than expected genetic diversity (i.e. contrasted with expectations of a severe genetic bottleneck upon a single invasion) if seeds from multiple plants continually became established (e.g. Sakai et al., 2001; Kolbe et al., 2004; Frankham, 2005; Dlugosch and Parker, 2007; Sutherland et al., 2021). Further, there is evidence that each putative invasion and subsequent spread led to long-distance dispersal within the invasive range over the last century, with "southern" mitotypes present as far north as central-western New York State (i.e. Tompkins County, New York), and "northern" mitotypes present as far south as eastern Tennessee (Fig. 5B). Indeed, samples collected in 2020 from the original site where stiltgrass was collected 101 years before (Knox County, Tennessee) revealed a mix of northern and southern mitotypes, suggesting that this species has been dispersed extensively over the past few decades via anthropogenic activity. This is significant, as such long-distance dispersal may lead to rapid admixture of previously separated genotypes from the native range, allowing the genomic potential for rapid adaptation to local conditions (Verhoeven et al., 2010; Rius and Darling, 2014), and thus presenting a mechanism for increased invasive potential over time (Dlugosch and Parker, 2008; Keller and Taylor, 2010; Dlugosch et al., 2015; Sutherland et al., 2021).

589 There is evidence that *M. vimineum* has experienced rapid adaptation after becoming established
590 in the invasive range, in terms of flowering phenology across a latitudinal gradient, and
591 growth/reproductive advantages of invasive populations compared with those in the native range,
592 in line with the Evolution of Increased Competitive Ability hypothesis (Flory et al., 2011; Novy
593 et al., 2013; Huebner et al., 2022). Barrett et al (2022) suggested that this may further extend to
594 selection in the invasive range for different awn phenotypes. In the eastern US, there is a strong
595 latitudinal pattern of awnless forms in the South, long-awned forms in the North, and
596 intermediate- or short-awned forms at mid-latitudes. A similar but relatively weaker pattern was
597 observed in Asia, with both awned and awnless phenotypes intermixed at low and mid-latitudes,
598 but a predominance of awned forms at higher latitudes. Awns are hypothesized to aid in
599 microsite dispersal and burial via hygroscopic movement, effectively drilling the seed-containing
600 floret into the seed bank (Cavanagh et al., 2020). Awns are expected to play a role in seedling
601 burial and increased survival from frequent and intense soil freezing events at higher latitudes.
602 Our mitochondrial SNP analysis (Fig. 5B), and previous analysis of nuclear SNP variation
603 (Barrett et al., 2022), support a scenario consistent with intensified, post-invasion selection for
604 awn phenotypes in the eastern US, favoring awnless forms at lower latitudes and awned forms at
605 higher latitudes. Habitat filtering may have also played a role (Weiher and Keddy, 1995), by
606 selecting which phenotypes were successful in their initial invasions, with a higher likelihood of
607 successful invasion hypothesized in the South by awnless forms, and by awned forms in the
608 North. We are currently conducting burial, germination, and seed survival experiments to test
609 hypotheses on selection for awn phenotypes in the invasive range.
610

611 Genome sequencing efforts in invasive plant species are in their infancy, but hold great potential
612 for the identification, phylogenetic placement, evolutionary ecology, and management of these
613 species. High-quality genome sequences and annotations provide much needed baseline data,
614 enabling subsequent studies of invasion routes, invasion history, and other diverse applications in
615 invasion biology. Here we have sequenced a reference mitogenome for *M. vimineum*, one of the
616 most damaging invasive plants in North America, to aid in such future studies. While
617 characterizing genome structure and content, we also corroborated recent studies on the complex
618 invasion history and spatiotemporal patterns of mitogenomic variation in the native and invasive
619 ranges. Most importantly, such genomic resources will aid in efforts to predict ongoing patterns
620 of spread within this species, responses to climate change, and possibly help predict future
621 threats from other invasive species, allowing genomically informed forecasting.
622

623 **Author contributions**

624

625 CFB conceived the study, analyzed data, and led the writing of the manuscript. KS, W-BY, and
626 C-HC provided Asian samples, and contributed to drafts of the manuscript. DR and BTS
627 analyzed data and helped draft the manuscript. CDH collected seed, maintained plants in a
628 controlled environment (growth chamber), and helped draft the manuscript. CWC generated
629 data, assisted with data analyses, and helped draft the manuscript. All authors have reviewed and
630 approved the final manuscript.
631

632 **Acknowledgments**

633

This work was supported by the US National Science Foundation (award OIA-1920858), the West Virginia University Department of Biology, and the USDA Forest Service Northern Research Station. The authors thank Mark Daly, Jasmine Haimovitz, Joanna Gallagher, and Jordan Zhang at Dovetail Genomics, LLC (Cantata Bio, LLC) for expert assistance with long-read sequencing, and GeneWiz, Inc. for RNA sequencing. We thank J. Beck, M. Latvis, N. Kooyers, M. McKain, E. Sigel, and B. Sutherland for feedback and discussion. We thank the following collaborators for providing contemporary field-collected material: M. McKain, G. Matlack, G. Moore, S. Kuebbing, B. Molano-Flores, A. Kennedy, J. Fagan, N. Koenig, P. Crim, G. Scott, B. Foster, M. Heberling, A. Bowe, P. Wolf, K. Willard, and J. McNeal. For access to herbarium collections we thank: Tiana Rehman (BRIT), Bonnie Isaac (CM), Mason Heberling (CM), John Freudenstein (OS), Anna Statler (BH), Tanya Livshultz (PH), Meghann Toner (US), Lauren Boyle (MO), Margaret Oliver (TENN), and Donna Ford-Werntz (WVA). For assistance with genomic sequencing, we thank R. Percifield, D. Primerano, and J. Fan. For collections in Japan, we thank C. Hara, S. Mori, M. Sato, T. Shimizu, and K. Tanaka. We thank the WVU Genomics Core Facility for support provided to help make this publication possible and for CTSI Grant no. U54 GM104942, which in turn provides financial support to the WVU Core Facility. We further acknowledge WV-INBRE (P20GM103434), a COBRE ACCORD grant (1P20GM121299), and a West Virginia Clinical and Translational Science Institute (WV-CTSI) grant (2U54GM104942) in supporting the Marshall University Genomics Core (Research Citation: Marshall University Genomics Core Facility, RRID:SCR_018885).

Literature Cited

Adobe Inc. 2019 Adobe Illustrator. Retrieved from https://adobe.com/products/illustrator.

657 Alverson AJ, DW Rice, S Dickinson, K Barry, JD Palmer 2011 Origins and recombination of the
658 bacterial-sized multichromosomal mitochondrial genome of cucumber. Plant Cell
659 23:2499–2513.

660 Alverson AJ, X Wei, DW Rice, DB Stern, K Barry, JD Palmer 2010 Insights into the evolution
661 of mitochondrial genome size from complete sequences of *Citrullus lanatus* and
662 *Cucurbita pepo* (Cucurbitaceae). Mol Biol Evol 27:1436–1448.

663 Amos B, C Aurrecoechea, M Barba, A Barreto, EY Basenko, W Bażant, R Belnap, AS Blevins,
664 U Böhme, J Brestelli, et al. 2022 VEuPathDB: the eukaryotic pathogen, vector and host
665 bioinformatics resource center. Nucleic Acids Res 50:D898–D911.

666 Arthan W, MR McKain, P Traiperm, CAD Welker, JK Teisher, EA Kellogg 2017
667 Phylogenomics of Andropogoneae (Panicoideae: Poaceae) of Mainland Southeast Asia.
668 Syst Bot 42:418–431.

669 Banerjee AK, W Guo, Y Huang 2019 Genetic and epigenetic regulation of phenotypic variation
670 in invasive plants – linking research trends towards a unified framework. NeoBiota
671 49:77–103.

672 Bao W, KK Kojima, O Kohany 2015 Repbase Update, a database of repetitive elements in
673 eukaryotic genomes. Mobile DNA 6:11.

674 Barrett CF, WJ Baker, JR Comer, JG Conran, SC Lahmeyer, JH Leebens□Mack, J Li, GS Lim,
675 DR Mayfield□Jones, L Perez, et al. 2016 Plastid genomes reveal support for deep
676 phylogenetic relationships and extensive rate variation among palms and other
677 commelinid monocots. New Phytol 209:855–870.

678 Barrett CF, CD Huebner, ZA Bender, TA Budinsky, CW Corbett, M Latvis, MR McKain, M
679 Motley, SV Skibicki, HL Thixton, et al. 2022 Digitized collections elucidate invasion
680 history and patterns of awn polymorphism in *Microstegium vimineum*. Am J Bot
681 109:689–705.

682 Bendich AJ 1993 Reaching for the ring: the study of mitochondrial genome structure. Curr Genet
683 24:279–290.

684 Bieker VC, P Battlay, B Petersen, X Sun, J Wilson, JC Brealey, F Bretagnolle, K Nurkowski, C
685 Lee, FS Barreiro, et al. 2022 Uncovering the genomic basis of an extraordinary plant
686 invasion. Sci Adv 8:eabo5115.

687 van Boheemen LA, E Lombaert, KA Nurkowski, B Gauffre, LH Rieseberg, KA Hodgins 2017
688 Multiple introductions, admixture and bridgehead invasion characterize the introduction
689 history of *Ambrosia artemisiifolia* in Europe and Australia. Mol Ecol 26:5421–5434.

690 Camacho C, G Coulouris, V Avagyan, N Ma, J Papadopoulos, K Bealer, TL Madden 2009
691 BLAST+: architecture and applications. BMC Bioinform 10:421.

692 Cardi T, P Giegé, S Kahlau, N Scotti 2012 Expression profiling of organellar genes. In: Bock R,
693 Knoop V, editors. Genomics of chloroplasts and mitochondria. Pages 323–355 *In*
694 Advances in photosynthesis and respiration. Vol. 35. Springer Netherlands, Dordrecht.

695 Cavanagh AM, JW Morgan, RC Godfree 2020 Awn morphology influences dispersal, microsite
696 selection and burial of Australian native grass diaspores. Front Ecol Evol 8. [accessed
697 2023 Feb 7]. https://www.frontiersin.org/articles/10.3389/fevo.2020.581967

698 Chen C-H, JF Veldkamp, C-S Kuoh, C-C Tsai, Y-C Chiang 2009 Segregation of *Leptatherum*
699 from *Microstegium* (Andropogoneae, Poaceae) confirmed by Internal Transcribed Spacer
700 DNA sequences. Blumea 54:175–180.

701 Chen C-H, J-F Veldkamp, C-S Kuoh 2012 Taxonomic revision of *Microstegium* s.str.
702 (Andropogoneae, Poaceae). Blumea 57:160–189.

703 Clifton SW, P Minx, CM-R Fauron, M Gibson, JO Allen, H Sun, M Thompson, WB Barbazuk,
704 S Kanuganti, C Tayloe, et al. 2004 Sequence and comparative analysis of the maize NB
705 mitochondrial genome. Plant Physiol 136:3486–3503.

706 Crotty SM, BQ Minh, NG Bean, BR Holland, J Tuke, LS Jermiin, AV Haeseler 2020 GHOST:
707 Recovering historical signal from heterotachously evolved sequence alignments. Syst
708 Biol 69:249–264.

709 Daehler CC 1998 The taxonomic distribution of invasive angiosperm plants: Ecological insights
710 and comparison to agricultural weeds. Biol Conserv 84:167–180.

711 Dlugosch KM, IM Parker 2008 Founding events in species invasions: genetic variation, adaptive
712 evolution, and the role of multiple introductions. Mol Ecol 17:431–449.

713 Dlugosch KM, FA Cang, BS Barker, K Andonian, SM Swope, LH Rieseberg 2015 Evolution of
714 invasiveness through increased resource use in a vacant niche. Nat Plants 1:15066.

715 Doyle JJ, JL Doyle 1987 A rapid DNA isolation procedure for small quantities of fresh leaf
716 tissue. Phytochemical Bulletin, 19:11-15.

717 Estep MC, MR McKain, D Vela Diaz, J Zhong, JG Hodge, TR Hodkinson, DJ Layton, ST
718 Malcomber, R Pasquet, EA Kellogg 2014 Allopolyploidy, diversification, and the
719 Miocene grassland expansion. PNAS 111:15149–15154.

720 Fairbrothers DE, JR Gray 1972 *Microstegium vimineum* (Trin.) *A. Camus* (Gramineae) in the
721 United States. J Torrey Bot 99:97-100.

722 Fang Y, H Wu, T Zhang, M Yang, Y Yin, L Pan, et al. 2012 A complete sequence and
723 transcriptomic analyses of date palm (*Phoenix dactylifera L.*) mitochondrial genome.
724 PLoS ONE 7: e37164.

725 Finch DM, JL Butler, JB Runyon, CJ Fettig, FF Kilkenny, S Jose, SJ Frankel, SA Cushman, RC
726 Cobb, JS Dukes, et al. 2021 Effects of climate change on invasive species. Pages 57–83
727 *In* Poland TM, Patel-Weynand T, Finch DM, Miniat CF, Hayes DC, Lopez VM, eds.
728 Invasive species in forests and rangelands of the United States. Cham: Springer
729 International Publishing. [accessed 2023 Feb 1]. https://link.springer.com/10.1007/978-3-
730 030-45367-1_4

731 Flory SL, F Long, K Clay 2011 Invasive *Microstegium* populations consistently outperform
732 native range populations across diverse environments. Ecology 92:2248–2257.

733 Frankham R 2005 Resolving the genetic paradox in invasive species. Heredity 94:385–385.

734 Givnish TJ, M Ames, JR McNeal, MR McKain, PR Steele, CW dePamphilis, SW Graham, JC
735 Pires, DW Stevenson, WB Zomlefer, et al. 2010 Assembling the Tree of the
736 Monocotyledons: plastome sequence phylogeny and evolution of Poales. Ann Missouri
737 Bot Gard 97:584–616.

738 Gualberto JM, D Mileshina, C Wallet, AK Niazi, F Weber-Lotfi, A Dietrich 2014 The plant
739 mitochondrial genome: dynamics and maintenance. Biochimie 100:107–120.

740 Harris RS 2007 Improved pairwise alignment of genomic DNA. Ph.D. Thesis, The Pennsylvania
741 State University.

742 Hawkins JS, D Ramachandran, A Henderson, J Freeman, M Carlise, A Harris, Z Willison-
743 Headley 2015 Phylogenetic reconstruction using four low-copy nuclear loci strongly
744 supports a polyphyletic origin of the genus *Sorghum*. Ann Bot 116:291–299.

745 Hoang DT, O Chernomor, A von Haeseler, BQ Minh, LS Vinh 2018 UFBoot2: Improving the
746 ultrafast bootstrap approximation. Mol Biol and Evol 35:518–522.

747 Hodgins KA, L Rieseberg, SP Otto 2009 Genetic control of invasive plants species using selfish
748 genetic elements. Evol Appl 2:555–569.

749 Holec S, H Lange, K Kühn, M Alioua, T Börner, D Gagliardi 2006 Relaxed transcription in
750 *Arabidopsis* mitochondria is counterbalanced by RNA stability control mediated by
751 polyadenylation and polynucleotide phosphorylase. Mol Cell Biol 26:2869–2876.

752 Hu J, Y Zheng, X Shang 2018 MiteFinderII: a novel tool to identify miniature inverted-repeat
753 transposable elements hidden in eukaryotic genomes. BMC Medical Genom 11:101.

754 Hudson J, JC Castilla, PR Teske, LB Beheregaray, ID Haigh, CD McQuaid, M Rius 2021
755 Genomics-informed models reveal extensive stretches of coastline under threat by an
756 ecologically dominant invasive species. PNAS 118:e2022169118.

757 Huebner CD 2010a Establishment of an invasive grass in closed-canopy deciduous forests across
758 local and regional environmental gradients. Biol Invasions 12:2069–2080.

759 Huebner CD 2010b Spread of an invasive grass in closed-canopy deciduous forests across local
760 and regional environmental gradients. Biol Invasions 12:2081–2089.

761 Huebner CD, CW Cameron Corbett, L Ferrari, LE Kosslow, SV Skibicki, CF Barrett 2022 Traits
762 that define invasiveness in *Microstegium vimineum* (Japanese stiltgrass) at local and
763 regional scales. Botany 2022, Anchorage, Alaska, United States.

764 Hunt M, ND Silva, TD Otto, J Parkhill, JA Keane, SR Harris 2015 Circlator: automated
765 circularization of genome assemblies using long sequencing reads. Genome Biol 16:294.

766 Jackman SD, L Coombe, RL Warren, H Kirk, E Trinh, T MacLeod, S Pleasance, P Pandoh, Y
767 Zhao, RJ Coope, et al. 2020 Complete mitochondrial genome of a gymnosperm, sitka
768 spruce (*Picea sitchensis*), indicates a complex physical structure. Genome Biol Evol
769 12:1174–1179.

770 Johnson DJ, SL Flory, A Shelton, C Huebner, K Clay 2015 Interactive effects of a non-native
771 invasive grass *Microstegium vimineum* and herbivore exclusion on experimental tree
772 regeneration under differing forest management. J Appl Ecol 52:210–219.

773 Kalyaanamoorthy S, BQ Minh, TKF Wong, A von Haeseler, LS Jermiin 2017 ModelFinder: fast
774 model selection for accurate phylogenetic estimates. Nat Methods 14:587–589.

775 Kassambara A 2020 ggpubr: 'ggplot2' based publication ready plots. R package version 0.4.0.
776 https://CRAN.R-project.org/package=ggpubr.

777 Keller SR, DR Taylor 2010 Genomic admixture increases fitness during a biological invasion. J
778 Evol Biol 23:1720–1731.

779 Kerns BK, C Tortorelli, MA Day, T Nietupski, AMG Barros, JB Kim, MA Krawchuk 2020
780 Invasive grasses: A new perfect storm for forested ecosystems? For Ecol Manag
781 463:117985.

782 Knoop V, M Unseld, J Marienfeld, P Brandt, S Sünkel, H Ullrich, A Brennicke 1996 Copia-,
783 Gypsy- and LINE-Like retrotransposon fragments in the mitochondrial genome of
784 *Arabidopsis thaliana*. Genetics 142:579–585.

785 Kolbe JJ, RE Glor, L Rodríguez Schettino, AC Lara, A Larson, JB Losos 2004 Genetic variation
786 increases during biological invasion by a Cuban lizard. Nature 431:177–181.

787 Kolmogorov M, J Yuan, Y Lin, PA Pevzner 2019 Assembly of long, error-prone reads using
788 repeat graphs. Nat Biotechnol 37:540–546.

789 Koren S, BP Walenz, K Berlin, JR Miller, NH Bergman, AM Phillippy 2017 Canu: scalable and
790 accurate long-read assembly via adaptive *k*-mer weighting and repeat separation. Genome
791 Res 27:722–736.

792 Kovar L, M Nageswara-Rao, S Ortega-Rodriguez, DV Dugas, S Straub, R Cronn, SR Strickler,
793 CE Hughes, KA Hanley, DN Rodriguez, et al. 2018 PacBio-based mitochondrial genome
794 assembly of *Leucaena trichandra* (Leguminosae) and an intrageneric assessment of
795 mitochondrial RNA editing. Genome Biol Evol 10:2501–2517.

796 Kurtz S 2001 REPuter: the manifold applications of repeat analysis on a genomic scale. Nucleic
797 Acids Res 29:4633–4642.

798 Lehwark P, S Greiner 2019 GB2sequin - A file converter preparing custom GenBank files for
799 database submission. Genomics 111:759–761.

800 Li H, B Handsaker, A Wysoker, T Fennell, J Ruan, N Homer, G Marth, G Abecasis, R Durbin,
801 1000 Genome Project Data Processing Subgroup 2009 The sequence alignment/map
802 format and SAMtools. Bioinformatics 25:2078–2079.

803 Lin Y, P Li, Y Zhang, D Akhter, R Pan, Z Fu, M Huang, X Li, Y Feng 2022 Unprecedented
804 organelle genomic variations in morning glories reveal independent evolutionary
805 scenarios of parasitic plants and the diversification of plant mitochondrial complexes.
806 BMC Biol 20:49.

807 Lloyd Evans D, SV Joshi, J Wang 2019 Whole chloroplast genome and gene locus phylogenies
808 reveal the taxonomic placement and relationship of *Tripidium* (Panicoideae:
809 Andropogoneae) to sugarcane. BMC Evol Biol 19:33.

810 Ma J, JL Bennetzen 2004 Rapid recent growth and divergence of rice nuclear genomes. PNAS
811 101:12404–12410.

812 Maier RM, P Zeitz, H Kössel, G Bonnard, JM Gualberto, JM Grienenberger 1996 RNA editing
813 in plant mitochondria and chloroplasts. Plant Mol Biol 1996 32:343-65

814 Marienfeld J, M Unseld, A Brennicke 1999 The mitochondrial genome of *Arabidopsis* is
815 composed of both native and immigrant information. Trends in Plant Sci 4:495–502.

816 Matheson P, A McGaughran 2022 Genomic data is missing for many highly invasive species,
817 restricting our preparedness for escalating incursion rates. Sci Rep 12:13987.

818 Mehrhoff LJ 2000 Perennial *Microstegium vimineum* (Poaceae): An apparent misidentification?
819 J Torrey Bot Soc 127:251.

820 Minh BQ, HA Schmidt, O Chernomor, D Schrempf, MD Woodhams, A von Haeseler, R Lanfear
821 2020 IQ-TREE 2: New models and efficient methods for phylogenetic inference in the
822 genomic era. Teeling E, editor. Mol Biol Evol 37:1530–1534.

823 Mortensen DA, ESJ Rauschert, AN Nord, BP Jones 2009 Forest roads facilitate the spread of
824 invasive plants. Invasive Plant Cci Manag 2:191–199.

825 Mounger J, ML Ainouche, O Bossdorf, A Cavé-Radet, B Li, M Parepa, A Salmon, J Yang, CL
826 Richards Epigenetics and the success of invasive plants. Philos Trans R Soc Lond B Biol
827 Sci 376:20200117.

828 Mower JP, DB Sloan, AJ Alverson 2012 Plant mitochondrial genome diversity: the genomics
829 revolution. Pages 123–144 *In* Wendel JF, Greilhuber J, Dolezel J, Leitch IJ, editors. Plant
830 Genome Diversity Volume 1: Plant genomes, their residents, and their evolutionary
831 dynamics. Springer, Vienna.

832 North HL, A McGaughran, CD Jiggins 2021 Insights into invasive species from whole-genome
833 resequencing. Mol Ecol 30:6289–6308.

834 Notsu Y, S Masood, T Nishikawa, N Kubo, G Akiduki, M Nakazono, A Hirai, K Kadowaki
835 2002 The complete sequence of the rice (*Oryza sativa* L.) mitochondrial genome:

836 frequent DNA sequence acquisition and loss during the evolution of flowering plants.
837 Mol Gen Genomics 268:434–445.

838 Novy A, S l. Flory, JM Hartman 2013 Evidence for rapid evolution of phenology in an invasive
839 grass. J Evol Biol 26:443–450.

840 Ortiz EM 2019 vcf2phylip v2.0: convert a VCF matrix into several matrix formats for
841 phylogenetic analysis. DOI:10.5281/zenodo.2540861

842 Palmer JD, LA Herbon 1988 Plant mitochondrial DNA evolves rapidly in structure, but slowly in
843 sequence. J Mol Evol 28:87–97.

844 Pimentel D, R Zuniga, D Morrison 2005 Update on the environmental and economic costs
845 associated with alien-invasive species in the United States. Ecol Econ 52:273–288.

846 Poplin R, V Ruano-Rubio, MA DePristo, TJ Fennell, MO Carneiro, GA Van der Auwera, DE
847 Kling, LD Gauthier, A Levy-Moonshine, D Roazen, et al. 2017 Scaling accurate genetic
848 variant discovery to tens of thousands of samples. bioRxiv:201178.

849 Ramachandran D, CD Huebner, M Daly, J Haimovitz, T Swale, CF Barrett 2021 chromosome
850 level genome assembly and annotation of highly invasive Japanese stiltgrass
851 (*Microstegium vimineum*). Genome Biol Evol 13:evab238.

852 Ranwez V, EJP Douzery, C Cambon, N Chantret, F Delsuc 2018 MACSE v2: Toolkit for the
853 alignment of coding sequences accounting for frameshifts and stop codons. Mol Biol
854 Evol 35:2582–2584.

855 Rauschert ESJ, DA Mortensen, ON Bjørnstad, AN Nord, N Peskin 2010 Slow spread of the
856 aggressive invader, *Microstegium vimineum* (Japanese stiltgrass). Biol Invasions 12:563–
857 579.

858 Revolinski SR, PJ Maughan, CE Coleman, IC Burke 2022 Preadapted to adapt: underpinnings of
859 adaptive plasticity revealed by the downy brome genome. In Review. [accessed 2023 Feb
860 1]. https://www.researchsquare.com/article/rs-2050485/v1

861 Rice DW, AJ Alverson, AO Richardson, GJ Young, MV Sanchez-Puerta, J Munzinger, K Barry,
862 JL Boore, Y Zhang, CW dePamphilis, et al. 2013 Horizontal transfer of entire genomes
863 via mitochondrial fusion in the angiosperm *Amborella*. Science 342:1468–1473.

864 Rius M, JA Darling 2014 How important is intraspecific genetic admixture to the success of
865 colonising populations? Trends Ecol Evol 29:233–242.

866 Ruwe H, G Wang, S Gusewski, C Schmitz-Linneweber 2016 Systematic analysis of plant
867 mitochondrial and chloroplast small RNAs suggests organelle-specific mRNA
868 stabilization mechanisms. Nucleic Acids Res 44:7406–7417.

869 Sakai AK, FW Allendorf, JS Holt, DM Lodge, J Molofsky, KA With, S Baughman, RJ Cabin, JE
870 Cohen, NC Ellstrand, et al. 2001 The population biology of invasive species. Ann Rev of
871 Ecol Systematics 32:305–332.

872 Sanchez□Puerta MV, LE García, J Wohlfeiler, LF Ceriotti 2017 Unparalleled replacement of
873 native mitochondrial genes by foreign homologs in a holoparasitic plant. New Phytol
874 214:376–387.

875 Simberloff D, J-L Martin, P Genovesi, V Maris, DA Wardle, J Aronson, F Courchamp, B Galil,
876 E García-Berthou, M Pascal, et al. 2013 Impacts of biological invasions: what's what and
877 the way forward. Trends Ecol Evol 28:58–66.

878 Sinn BT, CF Barrett 2020 Ancient mitochondrial gene transfer between fungi and the orchids.
879 Mol Biol Evol 37:44–57.

880 Sinn BT, SJ Simon, MV Santee, SP DiFazio, NM Fama, CF Barrett 2022 ISSRseq: An
881 extensible method for reduced representation sequencing. Methods Ecol Evol, 13:668–
882 681.

883 Sloan DB 2013 One ring to rule them all? Genome sequencing provides new insights into the
884 'master circle' model of plant mitochondrial DNA structure. New Phytol 200:978–985.

885 Sloan DB, Z Wu 2014 History of plastid DNA insertions reveals weak deletion and AT mutation
886 biases in Angiosperm mitochondrial genomes. Genome Biol Evol 6:3210–3221.

887 Smit AFA, R Hubley, P Green 2013 RepeatMasker Open-4.0. http://www.repeatmasker.org.

888 Sutherland BL, CF Barrett, JB Beck, M Latvis, MR McKain, EM Sigel, NJ Kooyers 2021
889 Botany is the root and the future of invasion biology. Am J Bot 108:549–552.

890 Turner KG, KL Ostevik, CJ Grassa, LH Rieseberg 2021 Genomic analyses of phenotypic
891 differences between native and invasive populations of diffuse knapweed (*Centaurea*
892 *diffusa*). Frontiers Ecol Evol 8. [accessed 2023 Feb 1].
893 https://www.frontiersin.org/articles/10.3389/fevo.2020.577635

894 Van der Auwera GA, Carneiro M, Hartl C, Poplin R, del Angel G, Levy-Moonshine A, Jordan T,
895 Shakir K, Roazen D, Thibault J,et al. 2013 From FastQ data to high-confidence variant
896 calls: the genome analysis toolkit best practices pipeline. Curr Protoc Bioinformatics,
897 43:11.10.1-11.10.33.

898 Van der Auwera GA, BD O'Connor 2020 Genomics in the Cloud: Using Docker, GATK, and
899 WDL in Terra (1st Edition). O'Reilly Media.

900 Verhoeven KJF, M Macel, LM Wolfe, A Biere 2010 Population admixture, biological invasions
901 and the balance between local adaptation and inbreeding depression. Proc Royal Soc B
902 278:2–8.

903 Walker BJ, T Abeel, T Shea, M Priest, A Abouelliel, S Sakthikumar, CA Cuomo, Q Zeng, J
904 Wortman, SK Young, et al. 2014 Pilon: An integrated tool for comprehensive microbial
905 variant detection and genome assembly improvement. Wang J, editor. PLoS ONE
906 9:e112963.

907 Watson L, Dallwitz MJ 1994 The grass genera of the world. CAB International, Wallingford,
908 Oxfordshire, UK.

909 Weiher E, PA Keddy 1995 The assembly of experimental wetland plant communities. Oikos
910 73:323–335.

911 Welker CAD, MR McKain, MC Estep, RS Pasquet, G Chipabika, B Pallangyo, EA Kellogg
912 2020 Phylogenomics enables biogeographic analysis and a new subtribal classification of
913 Andropogoneae (Poaceae—Panicoideae). J Systematics Evol 58:1003–1030.

914 Wick RR, MB Schultz, J Zobel, KE Holt 2015 Bandage: interactive visualization of *de novo*
915 genome assemblies. Bioinformatics 31:3350–3352.

916 Wickham H 2016 ggplot2: elegant graphics for data analysis. Springer-Verlag New York. ISBN
917 978-3-319-24277-4, https://ggplot2.tidyverse.org.

918 Wickham H, R François, L Henry, K Müller, D Vaughan 2023 dplyr: A grammar of data
919 manipulation. https://dplyr.tidyverse.org, https://github.com/tidyverse/dplyr

920 Wood DE, J Lu, B Langmead 2019 Improved metagenomic analysis with Kraken 2. Genome
921 Biol 20:257.

922 Wu Z, JM Cuthbert, DR Taylor, DB Sloan 2015 The massive mitochondrial genome of the
923 angiosperm *Silene noctiflora* is evolving by gain or loss of entire chromosomes. PNAS
924 112:10185–10191.

925 Wu Z, X Liao, X Zhang, LR Tembrock, A Broz 2022 Genomic architectural variation of plant
926 mitochondria—A review of multichromosomal structuring. J Sytematics Evol 60:160–
927 168.

928 Xiong W, L He, J Lai, HK Dooner, C Du 2014 HelitronScanner uncovers a large overlooked
929 cache of Helitron transposons in many plant genomes. PNAS 111:10263–10268.

930 Xiong Yanli, Q Yu, Yi Xiong, J Zhao, X Lei, L Liu, W Liu, Y Peng, J Zhang, D Li, et al. 2022
931 The complete mitogenome of *Elymus sibiricus* and insights into its evolutionary pattern
932 based on simple repeat sequences of seed plant mitogenomes. Frontiers Plant Sci 12.
933 [accessed 2023 Feb 1]. https://www.frontiersin.org/articles/10.3389/fpls.2021.802321

934 Yu X, W Jiang, W Tan, X Zhang, X Tian 2020 Deciphering the organelle genomes and
935 transcriptomes of a common ornamental plant *Ligustrum quihoui* reveals multiple
936 fragments of transposable elements in the mitogenome. Int J Biol Macromolecules
937 165:1988–1999.

938 Zhao N, Y Wang, J Hua 2018 the roles of mitochondrion in intergenomic gene transfer in plants:
939 a source and a pool. Int J Mol Sci 19:547.

940 **Figure Legends**

941 **Figure 1**. **A**. Linear map of the *Microstegium vimineum* mitogenome assembly and annotation.
942 Scale = 10 kilobases (kb). **B**. Proposed mitogenome secondary structural model emphasizing a
943 single large inverted repeat. **C**. Proposed model emphasizing two large inverted repeats. IR1, IR2
944 = Inverted Repeat 1 and Inverted Repeat 2 (respectively); DR1 = large, direct repeat 1; L =
945 length of each region; numbers preceding '×' = mean coverage depth of each region in B. Note:
946 the genome in B and C is represented as a looped or circular structure, but the genome could not
947 be circularized with long read data.
948
949 **Figure 2**. **A**. Repeat distribution in the mitogenomes of five species of grasses within the tribe
950 Andropogoneae. Points represent repeats scaled by size; shapes represent the orientation of each
951 repeat. **B**. Alternative conformations of the mitogenome based on LASTZ alignments of
952 assemblies of eight randomized subsets of PacBio reads, relative to the genome model in Figure
953 1A. 'IR' = inverted repeat, 'DR' = direct repeat. Red lines = forward orientation, blue lines =
954 reverse orientation.
955

Figure 3. Plastid-like sequences in the mitogenomes of sequenced grass species.

Figure 4. A. Location and relative levels of expression (TPM, transcripts per million) for mitochondrial CDS (coding DNA sequences) and plastid-like sequences. **B**. Relative expression levels of mitochondrial CDS and **C**. plastid-like sequences. **D**. Numbers of putative RNA editing sites for each mitochondrial CDS (C →U on forward strand or G→A on reverse strand). **E**. Predicted amino acid changes at putative RNA editing sites per mitochondrial CDS.

Figure 5. **A**. Maximum likelihood phylogenetic tree based on a 7,019 bp alignment of mitochondrial CDS under the GHOST heterotachy model. Numbers above branches indicate bootstrap support. *Microstegium* species are in blue font, with *M. vimineum* in red. **B**. Maximum likelihood phylogenetic tree among mitochondrial haplotypes of *M. vimineum*. Colors indicate regions from which samples were collected (green = Japan, orange = China, purple = Taiwan, red = the southeastern US, blue = the northeastern US). 'A' indicates the presence of awned florets, and a lack thereof indicates a lack of awned florets. The numbers on the right list the year each sample was collected; all samples collected prior to 2019 came from herbarium specimens, indicated by '***'.

Appendix A1

Voucher information: Species, Accession, US County (if applicable), Region/State, Country, Herbarium Code, Collector, Collection Number. Herbarium Codes: BH (Bailey Hortorium Herbarium), BRIT (Botanical Research Institute of Texas), CM (Carnegie Museum of Natural

978 History), MO (Missouri Botanical Garden), OS (Ohio State University Herbarium), PH
979 (Academy of Natural Sciences), TENN (University of Tennessee Herbarium), WVA (West
980 Virginia University Herbarium).

981 *Microstegium nudum* (Trin.) A. Camus, M-nudum-CHN-Hubei-1980-83-S44, n/a, Hubei, China,
982 1980, CM, Bartholomew et al., s.n.; *Microstegium vimineum* (Trin.) A. Camus, CHN-Jiangxi-
983 1983-12-S7, n/a, Jiangxi, China, 1983, CM, Yao, 8711; *Microstegium vimineum* (Trin.) A.
984 Camus, 111-JPN-Fukuoka-KS630-S9, n/a, Fukuoka, Japan, 2019, WVA, Suetsugu, 630;
985 *Microstegium vimineum* (Trin.) A. Camus, 115-JPN-Fukuoka-KS636-S11, n/a, Fukuoka, Japan,
986 2019, WVA, Suetsugu, 636; *Microstegium vimineum* (Trin.) A. Camus, 116-JPN-Fukuoka-
987 KS637-S12, n/a, Fukuoka, Japan, 2019, WVA, Suetsugu, 637; *Microstegium vimineum* (Trin.)
988 A. Camus, 117-JPN-Fukuoka-KS638-S13, n/a, Fukuoka, Japan, 2019, WVA, Suetsugu, 638;
989 *Microstegium vimineum* (Trin.) A. Camus, 118-JPN-Fukuoka-KS639-S14, n/a, Fukuoka, Japan,
990 2019, WVA, Suetsugu, 639; *Microstegium vimineum* (Trin.) A. Camus, JPN-Fukuoka-1-109-
991 S58, n/a, Fukuoka, Japan, 2019, WVA, Suetsugu, 633; *Microstegium vimineum* (Trin.) A.
992 Camus, JPN-Fukuoka-KS627-30-S17, n/a, Fukuoka, Japan, 2019, WVA, Suetsugu, 627;
993 *Microstegium vimineum* (Trin.) A. Camus, JPN-Fukuoka-KS634-31-S18, n/a, Fukuoka, Japan,
994 2019, WVA, Suetsugu, 634; *Microstegium vimineum* (Trin.) A. Camus, JPN-Fukuoka-KS635-
995 32-S19, n/a, Fukuoka, Japan, 2019, WVA, Suetsugu, 635; *Microstegium vimineum* (Trin.) A.
996 Camus, JPN-Shizuoka-KS604-67-S28, n/a, Fukuoka, Japan, 2019, WVA, Suetsugu, 604;
997 *Microstegium vimineum* (Trin.) A. Camus, JPN-Hyogo-KS595-24-S11, n/a, Hyogo, Japan, 2019,
998 WVA, Suetsugu, 595; *Microstegium vimineum* (Trin.) A. Camus, JPN-Hyogo-KS599-25-S12,
999 n/a, Hyogo, Japan, 2019, WVA, Suetsugu, 599; *Microstegium vimineum* (Trin.) A. Camus, JPN-
1000 Kagoshima-KS624-28-S15, n/a, Kagoshima, Japan, 2019, WVA, Suetsugu, 624; *Microstegium*

vimineum (Trin.) A. Camus, JPN-Kagoshima-KS626-29-S16, n/a, Kagoshima, Japan, 2019, WVA, Suetsugu, 626; *Microstegium japonicum* (Miq.) Koidz., M-japonicum-JPN-Kyoto-1964-84-S45, n/a, Kansai, Japan, 1964, CM, Murata, 19181; *Microstegium vimineum* (Trin.) A. Camus, JPN-Kyoto-1966-11-S6, n/a, Kansai, Japan, 1966, CM, Murata, G., 19905; *Microstegium vimineum* (Trin.) A. Camus, 92-JPN-Nagano-1972-S4, n/a, Nagano, Japan, 1972, CM, Shimizu, T., 24216; *Microstegium vimineum* (Trin.) A. Camus, 120-JPN-Shiga-KS648-S16, n/a, Shiga, Japan, 2019, WVA, Suetsugu, 648; *Microstegium vimineum* (Trin.) A. Camus, JPN-Shiga-KS650-122-S61, n/a, Shiga, Japan, 2019, WVA, Suetsugu, 650; *Microstegium vimineum* (Trin.) A. Camus, JPN-Shiga-KS651-123-S62, n/a, Shiga, Japan, 2019, WVA, Suetsugu, 651; *Microstegium vimineum* (Trin.) A. Camus, JPN-Shiga-KS652-124-S63, n/a, Shiga, Japan, 2019, WVA, Suetsugu, 652; *Microstegium vimineum* (Trin.) A. Camus, JPN-Shiga-KS654-126-S65, n/a, Shiga, Japan, 2019, WVA, Suetsugu, 654; *Microstegium vimineum* (Trin.) A. Camus, JPN-Shiga-KS655-127-S66, n/a, Shiga, Japan, 2019, WVA, Suetsugu, 655; *Microstegium vimineum* (Trin.) A. Camus, JPN-Shiga-KS660-151-S76, n/a, Shiga, Japan, 2019, WVA, Suetsugu, 660; *Microstegium vimineum* (Trin.) A. Camus, JPN-Shiga-KS663-154-S79, n/a, Shiga, Japan, 2019, WVA, Suetsugu, 663; *Microstegium vimineum* (Trin.) A. Camus, JPN-Shiga-KS665-156-S81, n/a, Shiga, Japan, 2019, WVA, Suetsugu, 665; *Microstegium vimineum* (Trin.) A. Camus, JPN-Shizuoka-KS602-26-S13, n/a, Shizuoka, Japan, 2019, WVA, Suetsugu, 602; *Microstegium vimineum* (Trin.) A. Camus, JPN-Shizuoka-KS606-69-S30, n/a, Shizuoka, Japan, 2019, WVA, Suetsugu, 606; *Microstegium vimineum* (Trin.) A. Camus, JPN-Shizuoka-KS607-70-S31, n/a, Shizuoka, Japan, 2019, WVA, Suetsugu, 607; *Microstegium vimineum* (Trin.) A. Camus, JPN-Shizuoka-KS608-71-S32, n/a, Shizuoka, Japan, 2019, WVA, Suetsugu, 608; *Microstegium vimineum* (Trin.) A. Camus, JPN-Shizuoka-KS610-73-S34, n/a, Shizuoka, Japan, 2019, WVA,

Suetsugu, 610; *Microstegium vimineum* (Trin.) A. Camus, JPN-Shizuoka-KS611-74-S35, n/a, Shizuoka, Japan, 2019, WVA, Suetsugu, 611; *Microstegium vimineum* (Trin.) A. Camus, JPN-Shizuoka-KS612-27-S14, n/a, Shizuoka, Japan, 2019, WVA, Suetsugu, 612; *Microstegium vimineum* (Trin.) A. Camus, JPN-Iwate-1937-82-S43, n/a, Tohoku, Japan, 1937, CM, Iwabuchi, H., 5516; *Microstegium vimineum* (Trin.) A. Camus, TWN-N-21-11-S38, n/a, Nantou, Taiwan, 2020, WVA, Chen, TWN-N-21-11; *Microstegium vimineum* (Trin.) A. Camus, TWN-N-21-2-S29, n/a, Nantou, Taiwan, 2020, WVA, Chen, TWN-N-21-2; *Microstegium vimineum* (Trin.) A. Camus, TWN-N-21-5-S32, n/a, Nantou, Taiwan, 2020, WVA, Chen, TWN-N-21-5; *Microstegium vimineum* (Trin.) A. Camus, TWN-N-21-8-S35, n/a, Nantou, Taiwan, 2020, WVA, Chen, TWN-N-21-8; *Microstegium ciliatum* (Trin.) A. Camus, M-ciliatum-TWN-Pintung-1960-88-S49, n/a, Pintung, Taiwan, 2020, CM, Hsu, 1073; *Microstegium fauriei* (Hayata) Honda), M-fauriei-TWN-Taichung-1976-87-S48, n/a, Taichung, Taiwan, 2020, CM, Kuo, 7116; *Microstegium geniculatum* (Hayata) Honda, M-geniculatum-TWN-Taichung-1961-86-S47, n/a, Taichung, Taiwan, 2020, CM, Feung, 4439; *Microstegium glaberrimum* (Honda) Koidz., M-glaberinum-TWN-Taipei-1975-85-S46, n/a, Taipei, Taiwan, 2020, CM, Kuo, 6424; *Microstegium vimineum* (Trin.) A. Camus, AL-Cherokee-1969-S67, Cherokee, Alabama, USA, 2020, TENN, Kral, 37767; *Microstegium vimineum* (Trin.) A. Camus, AL-MAD-1-1-S51, Madison, Alabama, USA, 2020, WVA, Wolf, AL-MAD-1-1; *Microstegium vimineum* (Trin.) A. Camus, DE-New-Castle-1948-138-S68, New Castle, Delaware, USA, 1948, CM, Long, B., 68410; *Microstegium vimineum* (Trin.) A. Camus, GA-BAR-2-1-S55, Bartow, Georgia, USA, 2020, WVA, McNeal, GA-BAR-2-1; *Microstegium vimineum* (Trin.) A. Camus, IL-JOHN-2-1-S15, Johnson, Illinois, USA, 2020, WVA, Molano-Flores, IL-JOHN-2-1; *Microstegium vimineum* (Trin.) A. Camus, KY-McCreary3-1949-23-S10, McCreary, Kentucky, USA, 1949,

MO, Reed, 16339; *Microstegium vimineum* (Trin.) A. Camus, 215-MD-GR-1-5-S15, Alleghany, Maryland, USA, 2019, WVA, Huebner, MD-GR-1-5; *Microstegium vimineum* (Trin.) A. Camus, NJ-CUMB-1-1-S5, Cumberland, New Jersey, USA, 2020, WVA, Moore, NJ-CUMB-1-1; *Microstegium vimineum* (Trin.) A. Camus, NJ-CUMB-2-2-S6, Cumberland, New Jersey, USA, 2020, WVA, Moore, NJ-CUMB-2-2; *Microstegium vimineum* (Trin.) A. Camus, NY-Bronx-1991-140-S69, Bronx, New York, USA, 1991, CM, Nee, M., 41826; *Microstegium vimineum* (Trin.) A. Camus, NY-Thomkins-2004-S86, Tompkins, New York, USA, 2004, BH, , ; *Microstegium vimineum* (Trin.) A. Camus, NY-TOM-6M-1-1-S20, Tompkins, New York, USA, 2020, WVA, Bowe, NY-TOM-6M-101; *Microstegium vimineum* (Trin.) A. Camus, NY-TOM-IC-1-1-S18, Tompkins, New York, USA, 2020, WVA, Bowe, NY-TOM-IC-1-1; *Microstegium vimineum* (Trin.) A. Camus, NY-TOM-IC-1-6-S19, Tompkins, New York, USA, 2020, WVA, Bowe, NY-TOM-IC-1-6; *Microstegium vimineum* (Trin.) A. Camus, NC-Halifax-1956-50-S21, Halifax, North Carolina, USA, 1956, BRIT, Ahles, 20724; *Microstegium vimineum* (Trin.) A. Camus, NC-Yancey-1958-51-S22, Yancey, North Carolina, USA, 1958, BRIT, Ahles, 50776; *Microstegium vimineum* (Trin.) A. Camus, NC-Martin-1973-76-S37, Martin, North Carolina, USA, 1973, CM, Boufford, D.E., 12249; *Microstegium vimineum* (Trin.) A. Camus, NC-SP-2-1-S57, Mitchell, North Carolina, USA, 2020, WVA, Barrett, NC-SP-2-1; *Microstegium vimineum* (Trin.) A. Camus, OH-Adams-Co1-1948-4-S4, Adams, Ohio, USA, 1948, OS, Barley, F., s.n.; *Microstegium vimineum* (Trin.) A. Camus, OH-Adams-Co3-1954-5-S5, Adams, Ohio, USA, 1954, OS, Barley, F., s.n.; *Microstegium vimineum* (Trin.) A. Camus, OH-Adams-Co5-1971-1-S1, Adams, Ohio, USA, 1971, OS, Barley, F., s.n.; *Microstegium vimineum* (Trin.) A. Camus, OH-Adams-Co6-1971-2-S2, Adams, Ohio, USA, 1971, OS, Barley, F., s.n.; *Microstegium vimineum* (Trin.) A. Camus, 89-Brown-OH-1977-S1, Brown, Ohio, USA, 1977, OS, Cusick,

A.W., s.n.; *Microstegium vimineum* (Trin.) A. Camus, OH-Adams-Co7-1989-3-S3, Adams, Ohio, USA, 1989, OS, Barley, F., s.n.; *Microstegium vimineum* (Trin.) A. Camus, 91-Portage-OH-2010-S3, Portange, Ohio, USA, 2010, OS, Gardner, R.L., 6970; *Microstegium vimineum* (Trin.) A. Camus, OH-ATH-1-3-S1, Athens, Ohio, USA, 2020, WVA, Matlack, OH-ATH-1-3; *Microstegium vimineum* (Trin.) A. Camus, OH-ATH-2-4-S2, Athens, Ohio, USA, 2020, WVA, Matlack, OH-ATH-2-4; *Microstegium vimineum* (Trin.) A. Camus, OH-VIN-1-3-S12, Vinton, Ohio, USA, 2020, WVA, Scott, OH-VIN-1-3; *Microstegium vimineum* (Trin.) A. Camus, OH-VIN-2-1-S13, Vinton, Ohio, USA, 2020, WVA, Scott, OH-VIN-2-1; *Microstegium vimineum* (Trin.) A. Camus, PA-Berks-1940-233a-S37, Berks, Pennsylvania, USA, 1940, PH, Brumbach, 3277; *Microstegium vimineum* (Trin.) A. Camus, PA-Berks-1940-75-S36, Berks, Pennsylvania, USA, 1940, PH, Wilkens, 6471; *Microstegium vimineum* (Trin.) A. Camus, Bucks-1952-George-S45, Bucks, Pennsylvania, USA, 1952, PH, Long, 75812; *Microstegium vimineum* (Trin.) A. Camus, PA-Bucks-1954-26-S48, Bucks, Pennsylvania, USA, 1954, PH, Wherry, sn; *Microstegium vimineum* (Trin.) A. Camus, PA-Berks-1957b-S41, Berks, Pennsylvania, USA, 1957, PH, Wilkens, 9182; *Microstegium vimineum* (Trin.) A. Camus, PA-Berks-1959-S43, Berks, Pennsylvania, USA, 1959, PH, Berkheimer, 19765; *Microstegium vimineum* (Trin.) A. Camus, PA-Montgomery-1959-S42, Montgomery, Pennsylvania, USA, 1959, PH, Wherry, sn; *Microstegium vimineum* (Trin.) A. Camus, PA-Fulton-1995-79-S40, Fulton, Pennsylvania, USA, 1995, CM, Grund, 1392; *Microstegium vimineum* (Trin.) A. Camus, PA-ALLE-1-1-S7, Allegheny, Pennsylvania, USA, 2020, WVA, Kuebbing, PA-ALLE-1-1; *Microstegium vimineum* (Trin.) A. Camus, PA-BUT-1-1-S16, Butler, Pennsylvania, USA, 2020, WVA, Heberling, PA-BUT-1-1; *Microstegium vimineum* (Trin.) A. Camus, PA-MONT-1-1-S3, Montgomery, Pennsylvania, USA, 2020, WVA, Moore, PA-MONT-1-1; *Microstegium vimineum* (Trin.) A.

Camus, PR-ElVerdeExSta-1966-52-S23, Rio Grande, Puerto Rico, USA, 1966, BRIT, Duncan, sn; *Microstegium vimineum* (Trin.) A. Camus, TN-Anderson-1934-53-S24, Anderson, Tennessee, USA, 1934, TENN, Jennison, 4360; *Microstegium vimineum* (Trin.) A. Camus, TN-Anderson-1934-S61, Anderson, Tennessee, USA, 1934, BRIT, Jennison, 3348; *Microstegium vimineum* (Trin.) A. Camus, TN-Knox-1934-S65, Knox, Tennessee, USA, 1934, TENN, Miller, 3482; *Microstegium vimineum* (Trin.) A. Camus, TN-Knox-1936-16-S9, Knox, Tennessee, USA, 1936, MO, Jennison, 260; *Microstegium vimineum* (Trin.) A. Camus, TN-Roane-1956-S66, Roane, Tennessee, USA, 1956, TENN, Norris & DeSelm, 21779; *Microstegium vimineum* (Trin.) A. Camus, TN-Bount-1961-S62, Blount, Tennessee, USA, 1961, TENN, Pringle, 29862; *Microstegium vimineum* (Trin.) A. Camus, TN-Knox-1970-S74, Knox, Tennessee, USA, 1970, TENN, Somers & Bowers, 81; *Microstegium vimineum* (Trin.) A. Camus, TN-Roane-1974-80-S41, Roane, Tennessee, USA, 1974, CM, Hedge, 50096; *Microstegium vimineum* (Trin.) A. Camus, TN-Carrol-2007-S71, Carrol, Tennessee, USA, 2007, TENN, Crabtree & McCoy, sn; *Microstegium vimineum* (Trin.) A. Camus, TN-Cheatham-2010-S68, Cheatham, Tennessee, USA, 2010, TENN, Klagstad, 432; *Microstegium vimineum* (Trin.) A. Camus, TN-KNO-3C-2-1-S22, Knox, Tennessee, USA, 2020, WVA, Barrett, TN-KNO-3C-2-1-S22; *Microstegium vimineum* (Trin.) A. Camus, TN-KNO-3C-2-6-B-S44, Knox, Tennessee, USA, 2020, WVA, Barrett, TN-KNO-3C-2-6-B-S44; *Microstegium vimineum* (Trin.) A. Camus, TN-KNO-7I-2-1-B-S47, Knox, Tennessee, USA, 2020, WVA, Barrett, TN-KNO-7I-2-1-B-S47; *Microstegium vimineum* (Trin.) A. Camus, TN-KNO-HP-1-1-A-S24, Knox, Tennessee, USA, 2020, WVA, Barrett, TN-KNO-HP-1-1-A-S24; *Microstegium vimineum* (Trin.) A. Camus, TN-KNO-HP-1-1-B-S45, Knox, Tennessee, USA, 2020, WVA, Barrett, TN-KNO-HP-1-1-B-S45; *Microstegium vimineum* (Trin.) A. Camus, TN-KNO-HP-1-6-A-S25, Knox, Tennessee, USA, 2020, WVA,

Barrett, TN-KNO-HP-1-6-A-S25; *Microstegium vimineum* (Trin.) A. Camus, TN-KNO-HP-1-6-B-S46, Knox, Tennessee, USA, 2020, WVA, Barrett, TN-KNO-HP-1-6-B-S46; *Microstegium vimineum* (Trin.) A. Camus, TN-LPG-1-1-S59, Greene, Tennessee, USA, 2020, WVA, Barrett, TN-LPG-1-1-S59; *Microstegium vimineum* (Trin.) A. Camus, VA-Fairfax-1986-S80, Fairfax, Virginia, USA, 1986, TENN, Fosberg, 65307; *Microstegium vimineum* (Trin.) A. Camus, 206-VA-Bath-1-4-S8, Bath, Virginia, USA, 2019, WVA, Barrett, VA-BATH-1-4; *Microstegium vimineum* (Trin.) A. Camus, VA-SG-2-1-S49, Smyth, Virginia, USA, 2020, WVA, Barrett, VA-SMYTH-2-1; *Microstegium vimineum* (Trin.) A. Camus, VA-SG-2-6-S50, Smyth, Virginia, USA, 2020, WVA, Barrett, VA-SMYTH-2-6; *Microstegium vimineum* (Trin.) A. Camus, WV-Fayette-1977-105-S54, Fayette, West Virginia, USA, 1977, WVA, Grafton, sn; *Microstegium vimineum* (Trin.) A. Camus, 104-Cabell-Boone-WV-1987-S7, Cabell, West Virginia, USA, 1987, WVA, Cusick, 27164; *Microstegium vimineum* (Trin.) A. Camus, WV-Fayette-1997-103-S53, Fayette, West Virginia, USA, 1997, WVA, Grafton, sn; *Microstegium vimineum* (Trin.) A. Camus, WV-Calhoun-2000-96-S52, Calhoun, West Virginia, USA, 2000, WVA, Grafton, sn; *Microstegium vimineum* (Trin.) A. Camus, 99-WV-Clay-2002-S6, Clay, West Virginia, USA, 2002, WVA, Grafton, sn; *Microstegium vimineum* (Trin.) A. Camus, WV-Hardy-2003-107-S56, Hardy, West Virginia, USA, 2003, WVA, Grafton, sn; *Microstegium vimineum* (Trin.) A. Camus, WV-Harrison-2007-106-S55, Harrison, West Virginia, USA, 2007, WVA, Grafton, sn; *Microstegium vimineum* (Trin.) A. Camus, WV-Marion-2007-145-S74, Marion, West Virginia, USA, 2007, WVA, Grafton, sn; *Microstegium vimineum* (Trin.) A. Camus, WV-SR-2-3-225-S85, Preston, West Virginia, USA, 2019, WVA, Huebner & Barrett, WV-SR-2-1; *Microstegium vimineum* (Trin.) A. Camus, WI-LAC-2-1-S8, LaCrosse, Wisconsin, USA, 2020, WVA,

1138 Molano-Flores, WI-LAC-2-1; *Microstegium vimineum* (Trin.) A. Camus, WI-LAC-2-2-S9,

1139 LaCrosse, Wisconsin, USA, 2020, WVA, Molano-Flores, WI-LAC-2-2.

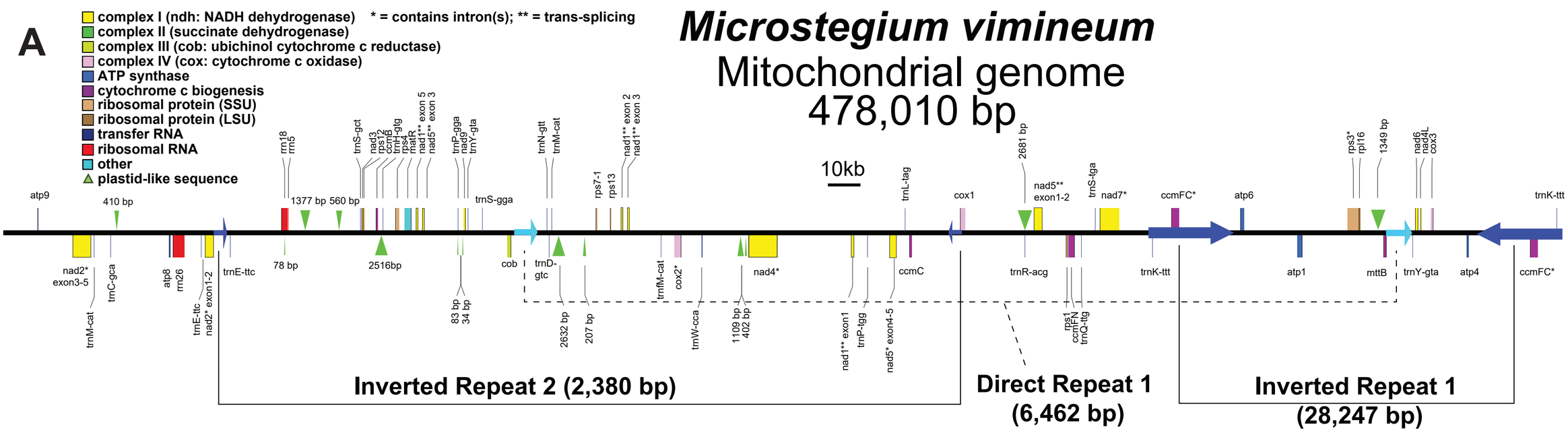

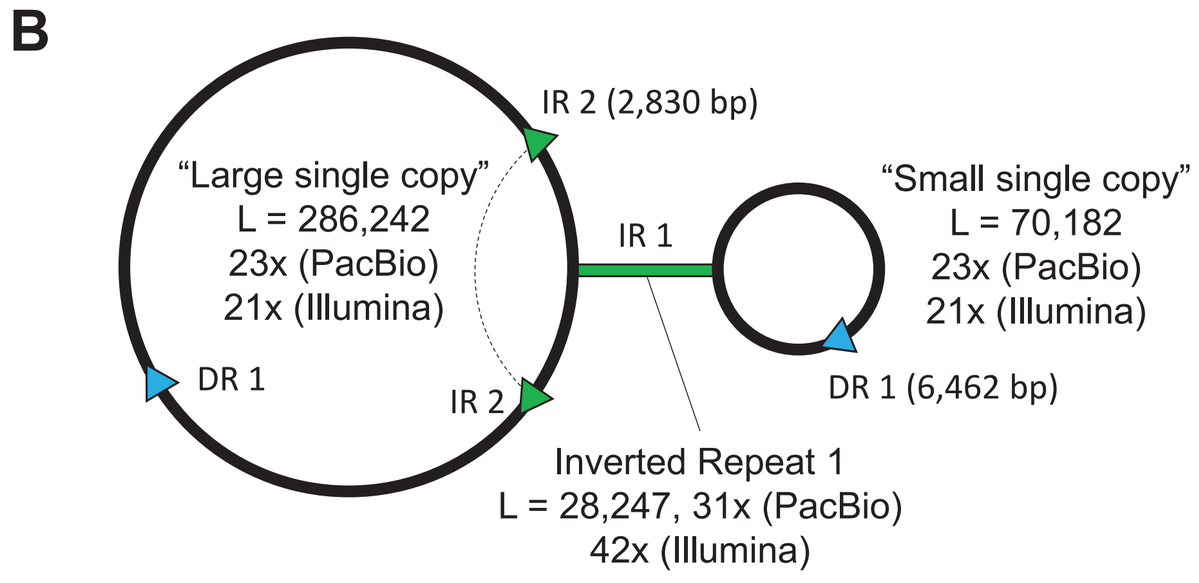

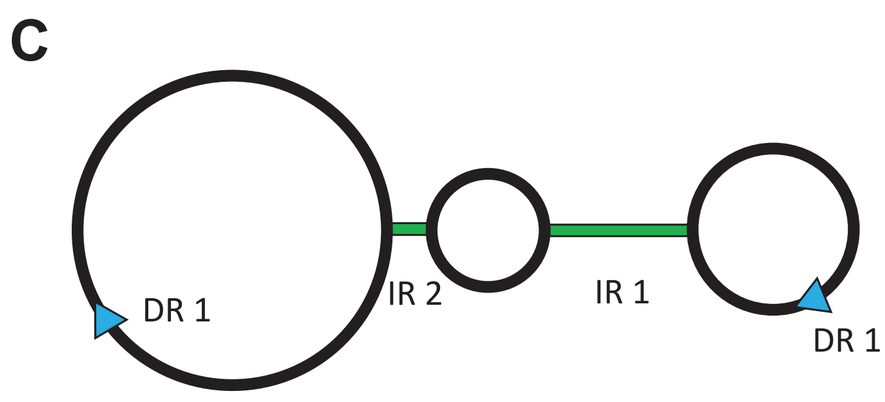

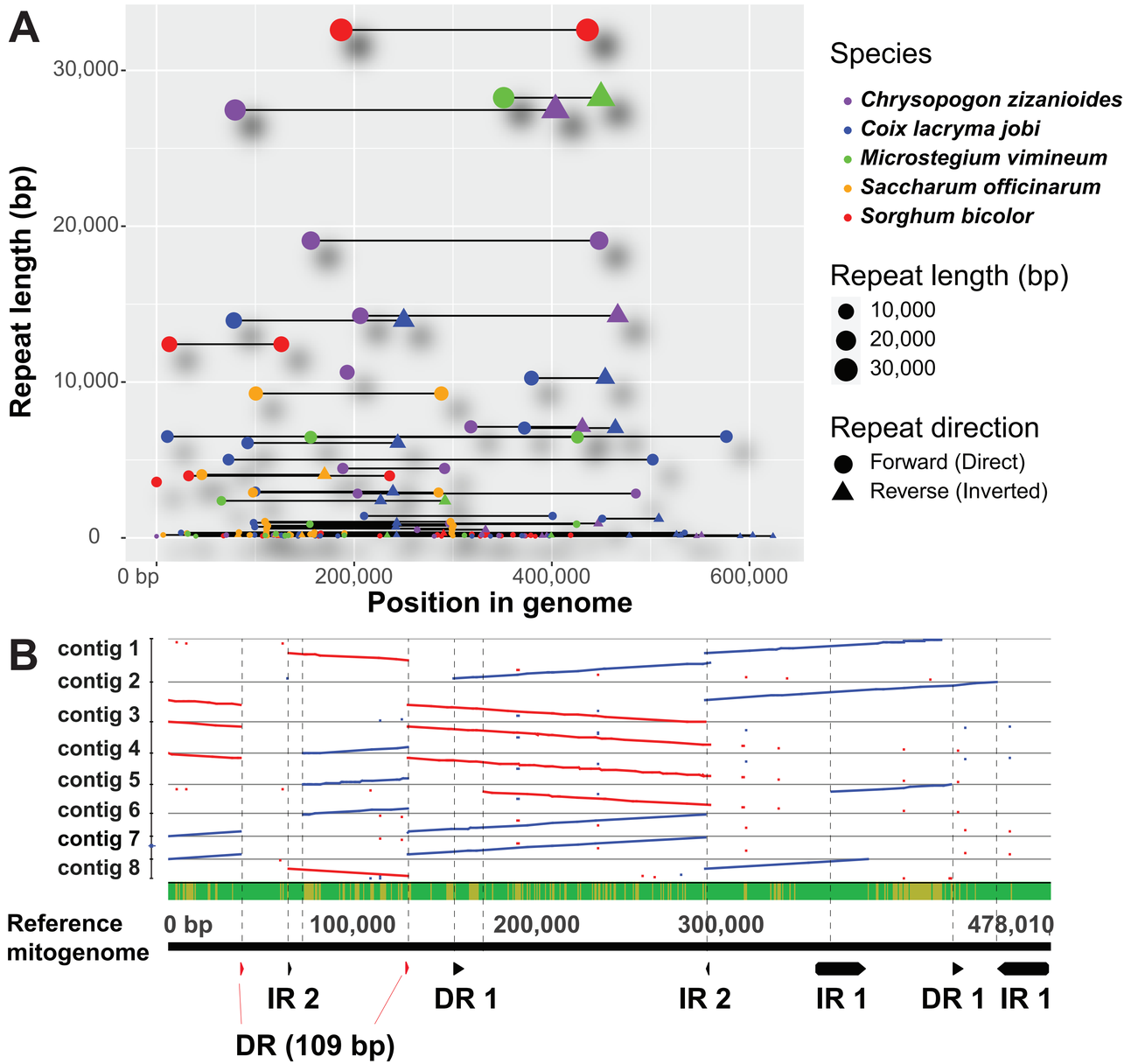

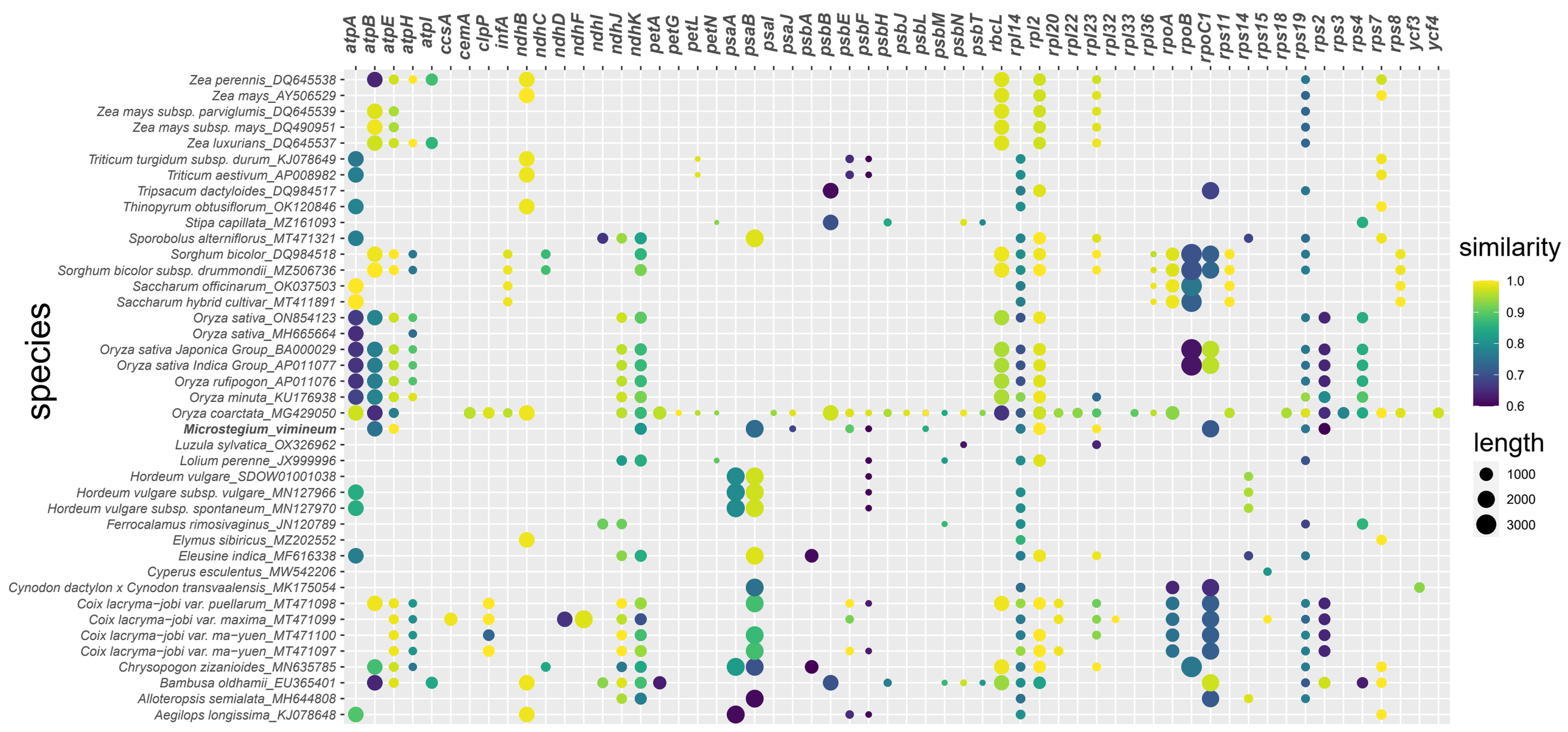
atpA
atpB
atpE
atpH
atpI
ccsA
cemA
clpP
infA
ndhB
ndhC
ndhD
ndhF
ndhI
ndhJ
ndhK
petA
petG
petL
petN
psaA
psaB
psaI
psaJ
psbA
psbB
psbE
psbF
psbH
psbJ
psbL
psbM
psbN
psbT
rbcL
rpl14
rpl2
rpl20
rpl22
rpl23
rpl32
rpl33
rpl36
rpoA
rpoB
rpoC1
rps11
rps14
rps15
rps18
rps19
rps2
rps3
rps4
rps7
rps8
ycf3
ycf4
species
Zea perennis_DQ645538
Zea mays_AY506529
Zea mays subsp. parviglumis_DQ645539
Zea mays subsp. mays_DQ490951
Zea luxurians_DQ645537
Triticum turgidum subsp. durum_KJ078649
Triticum aestivum_AP008982
Tripsacum dactyloides_DQ984517
Thinopyrum obtusiflorum_OK120846
Stipa capillata_MZ161093
Sporobolus alterniflorus_MT471321
Sorghum bicolor_DQ984518
Sorghum bicolor subsp. drummondii_MZ506736
Saccharum officinarum_OK037503
Saccharum hybrid cultivar_MT411891
Oryza sativa_ON854123
Oryza sativa_MH665664
Oryza sativa Japonica Group_BA000029
Oryza sativa Indica Group_AP011077
Oryza rufipogon_AP011076
Oryza minuta_KU176938
Oryza coarctata_MG429050
Microstegium_vimineum
Luzula sylvatica_OX326962
Lolium perenne_JX999996
Hordeum vulgare_SDOW01001038
Hordeum vulgare subsp. vulgare_MN127966
Hordeum vulgare subsp. spontaneum_MN127970
Ferrocalamus rimosivaginus_JN120789
Elymus sibiricus_MZ202552
Eleusine indica_MF616338
Cyperus esculentus_MW542206
Cynodon dactylon x Cynodon transvaalensis_MK175054
Coix lacryma−jobi var. puellarum_MT471098
Coix lacryma−jobi var. maxima_MT471099
Coix lacryma−jobi var. ma−yuen_MT471100
Coix lacryma−jobi var. ma−yuen_MT471097
Chrysopogon zizanioides_MN635785
Bambusa oldhamii_EU365401
Alloteropsis semialata_MH644808
Aegilops longissima_KJ078648
similarity
1.0
0.9
0.8
0.7
0.6
length
1000
2000
3000

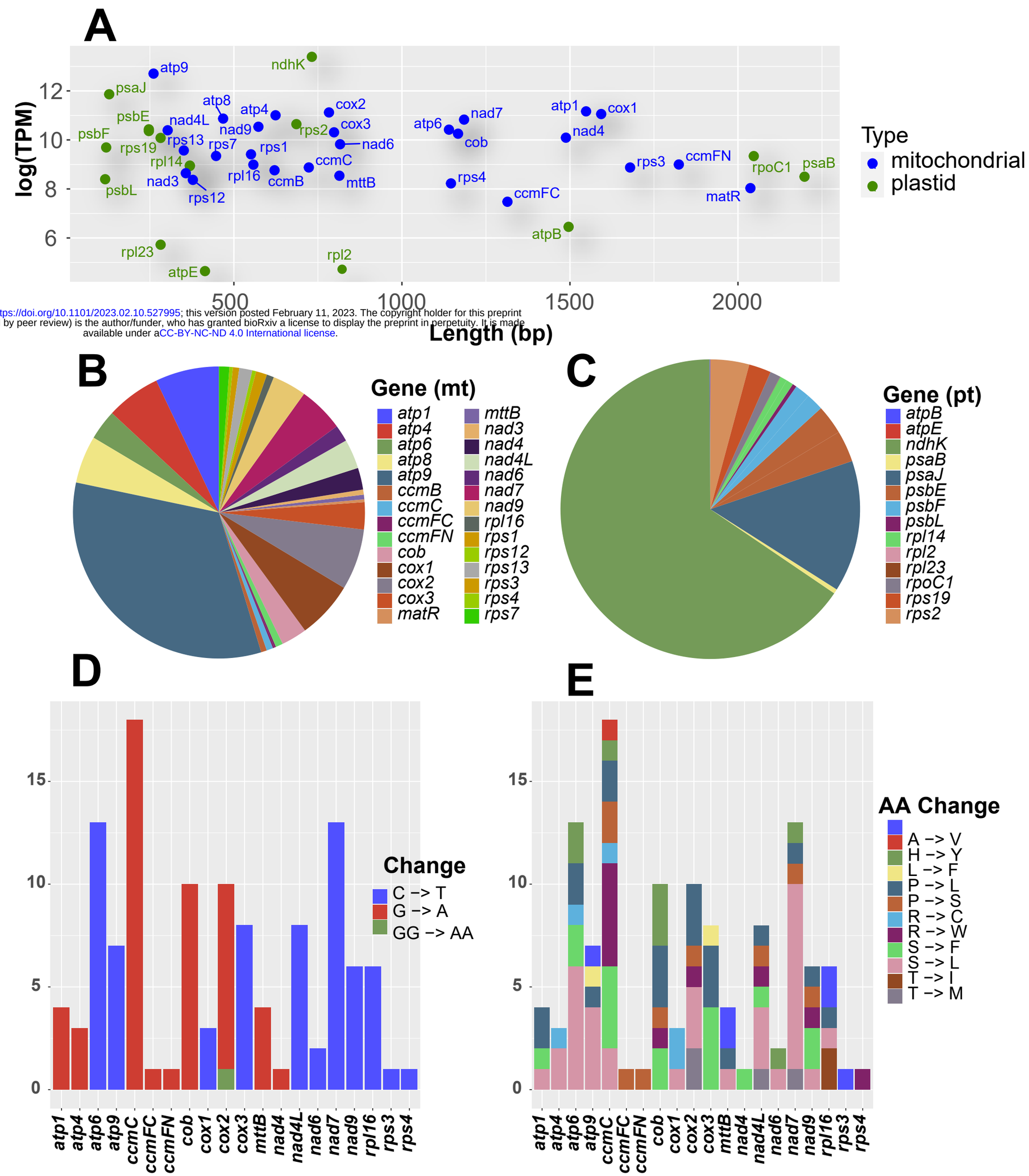

A

Cocos nucifera NC 031696
Phoenix dactylifera NC 016740
Vriesea hybrid cultivar OL840039
Cryptanthus acaulis OL839997
Neoregelia sp WH1915 OL840029
Sparganium confertum OL840034
Typha sp 11CS3675 OL840038
Rohrbachia minima OL840037
Typha lugdunensis OL840036
Mayaca fluviatilis OL840027
Mayaca fluviatilis OL840028
Xyris indica OL840040
Xyris pauciflora OL840041
Prionium serratum OL840031
Thurnia sphaerocephala OL840035
Isolepis setacea OL840018
Cyperus difformis OL839998
Cyperus esculentus MW542206
Juncus compressus OL840023
Juncus himalensis OL840025
Juncus alatus OL840022
Juncus grisebachii OL840024
Joinvillea ascendens OL840019
Joinvillea plicata OL840020
Joinvillea sp OL840021
Puelia olyriformis OL840032
Bambusa oldhamii EU365401
Ferrocalamus rimosivaginus JN120789
Lolium perenne JX999996
Hordeum vulgare subsp spontaneum MN127970
Hordeum vulgare subsp vulgare MN127966
Thinopyrum obtusiflorum OK120846
Triticum aestivum AP008982
Oryza coarctata MG429050
Oryza minuta KU176938
Oryza sativa Indica Group AP011077
Oryza rufipogon AP011076
Oryza sativa Japonica BA000029
Oryza sativa MH665664
Oryza sativa ON854123
Sporobolus alterniflorus MT471321
Eleusine indica MF616338
Cynodon dactylon x transvaalensis MK175054
Alloteropsis semialata MH644808
Tripsacum dactyloides DQ984517
Zea mays subsp parviglumis DQ645539
Zea luxurians DQ645537
Zea perennis DQ645538
Zea mays subsp mays DQ490951
Zea mays AY506529
Chrysopogon zizanioides MN635785
Saccharum hybrid cultivar MT411891
Saccharum officinarum OK037503
Microstegium nudum CHN-Hubei-1980
Sorghum bicolor subsp drummondii MZ506736
Sorghum bicolor DQ984518
Coix lacryma jobi var ma yuen MT471100
Coix lacryma jobi var maxima MT471099
Coix lacryma jobi var ma yuen MT471097
Coix lacryma jobi var puellarum MT471098
Microstegium faurei TWN Taichung
Microstegium sp Guangdong CHN-1-10
Microstegium ciliatum Pintung TWN 1960
Microstegium glaberinum TWN-Taipei-1975
Microstegium vimineum
Microstegium japonicum Kyoto JPN 1964
Microstegium sp Yunnan CHN 1-10

Poales
Arecales
Bromeliaceae
Typhaceae
Mayacaceae
Xyridaceae
Thurniaceae
Cyperaceae
Juncaceae
Joinvilleaceae
Poaceae
Tribe Andropogoneae

Microstegium spp.
M. vimineum

B

Microstegium vimineum

NE-US
SE-US
Taiwan
China
Japan

M. japonicum JPN Kyoto 1964 ***
M. nudum CHN Hubei 1980 ***
M. fauriei TWN Taichung 1976 ***
M. glaberinum TWN Taipei 1975 ***
M. ciliatum TWN Pintung 1960 ***
M. geniculatum TWN Taichung 1961 ***
TWN Nantou 21-1 A 2020
JPN Fukuoka 1 109 A 2019
JPN Shizuoka KS610 73 2019
JPN Fukuoka KS638 A 2019
JPN Fukuoka KS636 A 2019
JPN Fukuoka KS637 A 2019
JPN Shiga KS665 2019
WV Clay 2002 ***
JPN Shizuoka KS611 2019
TN Knox 7I 2-1B 2020
VA Smyth 2-1 2020
NC Mitchell 2-1 2020
JPN Fukuoka KS627 2019
Puerto Rico El Verde 1966 ***
AL Madison 1-1 2020
TN Knox HP 1-6B 2020
NC Yancey 1958 ***
NY Tompkins A 2004 ***
JPN Shiga KS660 151 A 2019
JPN Shizuoka KS602 26 A 2019
AL Cherokee 1969 ***
NC Halifax 1956 ***
NY Tompkins IC 1-1 A 2020
NY Tompkins IC 1-6 A 2020
TN Anderson 1934 ***
JPN Shizuoka KS604 A 2019
TN Roane 1974 ***
GA Bartow 2-1 2020
TN Knox HP 1-6A 2020
OH Adams 6 1971 ***
TN Blount 1961 ***
OH Adams 3 1954 ***
VA Smyth 2-6 2020
TN Roane 1956 ***
PA Berks A 1957 ***
TN Knox 1936 ***
TN Knox 1934 ***
TN Greene 1-1 2020
KY McCreary 3 1949 ***
NC Martin 1973 ***
OH Brown 1977 ***
JPN Shiga KS651 A 2019
TN Carrol 2007 ***
TN Knox 3C 2-6B 2020
WV Fayette2 CaneBranch 1977 ***
WV Fayette 1997 ***
JPN Shiga KS663 2019
OH Adams 7 1989 ***
OH Adams 5 1971 ***
OH Adams 1 1948 ***
NY Tompkins 6M 1-1 A 2020
TN Anderson 1934 ***
TN Cheatham 2010 ***
TN Knox 1970 ***
TN Knox HP 1-1B 2020
JPN Shizuoka KS606 A 2019
JPN Fukuoka KS635 A 2019
PA Bucks A 1954 ***
PA Montgomery A 1959 ***
DE New Castle A 1948 ***
WI LaCrosse 2-2 A 2020
JPN Shiga KS655 A 2019
NY Bronx A 1991 ***
OH Portage A 2010 ***
JPN Nagano A 1972 ***
WV Calhoun A 2000 ***
JPN Iwate A 1937 ***
OH Athens 1-3 A 2020
OH Vinton 2-1 2020
MD Allegheny 1-5 A 2020
WV Harrison A 2007 ***
PA Berks A 1959 ***
PA Fulton A 1995 ***
PA Berks A 1940 ***
PA Berks A 1940b***
JPN Shiga KS650 A 2019
JPN Shiga KS648 2019
NJ Cumberland 2-1 A 2020
JPN Fukuoka KS630 A 2019
JPN Shizuoka KS607 2019
VA Fairfax A 1986 ***
JPN Shizuoka KS608 2019
JPN Kagoshima KS624 2019
JPN Shizuoka KS612 A 2019
PA Allegheny 1-1 A 2020
IL Johnson 2-1 2020
TN Knox HP 1-1A 2020
OH Athens 2-4 A 2020
WV Hardy A 2003 ***
VA Bath 1-4 A 2019
WI LaCrosse 2-1 A 2020
JPN Hyogo KS595 2019
WV Preston 2-3 A 2019
CHN Jiangxi 1983 ***
NJ Cumberland 1-1 A 2020
TWN Nantou 21-5 2020
TN Knox 3C 2-1 2020
JPN Fukuoka KS639 A 2019
JPN Fukuoka KS634 A 2019
OH Vinton 1-3 2020
WV Marion A 2007 ***
PA Bucks A 1952 ***
PA Butler 1-1 A 2020
JPN Kagoshima KS626 2019
TWN Nantou 21-11 2020
TWN Nantou 21-8 2020
JPN Hyogo KS599 2019
PA Montgomery 1 1 A 2020
WV Cabell 1987 ***
JPN Shiga KS652 A 2019
JPN Kyoto 1966 ***
JPN Shiga KS654 2019